Title
ChI(r)P-seq: FoxP2 Binding Sites Uncover Molecular Mechanisms Influencing Songbird Vocalizations

Author
Kimball, Todd Haswell

Publication Date
2018

Peer reviewed|Thesis/dissertation

UNIVERSITY OF CALIFORINA

Los Angeles

ChI(r)P-seq: FoxP2 Binding Sites Uncover Molecular Mechanisms Influencing Songbird Vocalizations

A thesis submitted in partial satisfaction of the requirements for the degree Master of Science in Physiological Science

by

Todd Haswell Kimball

2018

ABSTRACT OF THE THESIS

ChI(r)P-seq: FoxP2 Binding Sites Uncover Molecular Mechanisms Influencing Songbird Vocalizations

by

Todd Haswell Kimball

Master of Science in Physiological Science

University of California, Los Angeles, 2018

Professor Stephanie Ann White, Chair

The zebra finch, like humans, share a vocal learning phenotype and are an ideal model system to understand the molecular underpinnings of this multigenomic trait. Gene expression profiles examined in zebra finch have painted a dynamic picture of the complex genetic interplay required to enable vocal learning. The transcription factor FoxP2 is a key contributor to the gene regulation necessary for vocal learning in both humans and zebra finch. Examining the genes FoxP2 targets may provide the first step in possible pathways necessary for vocal learning. Chromatin immunoprecipitation (ChIP) captures DNA-protein interactions, and by using this approach, we were able to demonstrate FoxP2 binding sites within the genome. ChIP-qPCR provided validation of our approach and evidence of FoxP2 binding to the promoter of *MAPK11*,

identified through our gene expression profile. Furthering this approach, ChIP-seq identified differential FoxP2 binding sites associated with developmental timepoints and sex differences, most notably Activating Transcription Factor 4 (*ATF4*), shown to influence synaptic plasticity and memory. The identification of FoxP2 binding sites and subsequent gene regulation will provide the starting point of pathways necessary for complex vocal development.

The thesis of Todd Haswell Kimball is approved.

Thomas J. O'Dell

Stephanie Correa Van Veen

Stephanie Ann White, Committee Chair

University of California, Los Angeles

2018

DEDICATION

To Blaire, who believes in me when I do not, who supports us when I could not, and who loves me for all that I am. Without you, this would not be possible, I love you.

To my mom, dad, brother and sisters, who still thought I was smart through all my dumb indecisions.

To everybody who has helped me find my way, I thank you. This is for ya'll.

Table of Contents

List of Tables

List of Figures

Acknowledgments

I am grateful to Dr. Stephanie White for all her encouragement, guidance, and freedom to come in and try to work my way through this field. All the members of the White lab that helped acclimate me to my new environment and introduced me to a field of science that made me curious of all different types of model systems and ways to investigate scientific enthusiasm. Thank you to my committee, Dr. Stephanie Correa and Dr. Tom O'Dell, for being supportive, kind, and understanding in our all too brief meetings.

Appendix 1 is a version of Burkett Z.D., Day N.F., Kimball T.H., Aamodt C.M., Heston J.B., Hilliard A.T., Xiao X, White S.A. FoxP2 isoforms delineate spatiotemporal transcriptional networks for vocal learning in the zebra finch. Elife. 2018 Jan 23;7. The authors thank Jennifer Morales and Maria Truong for their assistance in analyzing song and non-vocal behavior.

Introduction

As friends and family gathered to celebrate the marriage of two loved ones, a word of advice was asked from the couple who had been together the longest. After the ceremonial "She's always right" joke delighted the crowd, the following was offered, "The key to a healthy relationship is communication." The ability to effectively communicate thoughts and ideas provide an insight to one's knowledge, the ability to share information, and a window into how an individual's mind operates. Most have had the seemingly effortless experience of a shared conversation lasting hours, or the flip side, a painstaking, awkward few minutes. There are ways to study how to be a good communicator, tips to be engaging, to make an impact, and make our presence felt, but the underlying process of getting to that point is must be learned and practiced.

Effective communication begins by learning words and grammatical structure. Humans have the rare ability of vocal learning, the process of hearing vocalizations and learning how to produce them [1]. Babies are not born speaking, rather, by listening and processing auditory inputs (through interactions with adults), they are able to imitate those sounds. Eventually, one day, a child will be able to tell us what sound a dog makes. The progression from simple babbling to understanding the intricacies of language is remarkable, and its breadth of expressive capabilities is unmatched amongst other life on earth [2]. In an ideal setting, this development would be shared, but for some, vocal learning is disrupted and life is more difficult without effective communicative abilities.

The KE Family: Discovering a Molecular Link to Vocal Learning

In 1990, a case study brought to light a rare Mendelian inherited disorder affecting both speech production and comprehension in an English family, known as the KE family [3]. The

study diagnosed affected KE family members with developmental verbal dyspraxia (DVD), defined by a lack of articulation resulting from a deficiency in the planning, sequencing, and execution of the fine motor movements necessary for speech production. Contributing to the phenotype, the more cognitive aspects of language, including grammatical rules and syntactical structure, were also impaired, while their non-verbal IQ scores remained close to the population mean [4-7]. The physiological determinants underlying this particular speech deficit was localized to the basal ganglia, among other brain regions, with affected members displaying bilateral abnormalities in gray matter density [8-10]. While the physiological characterization of DVD was being characterized, the genetic basis underlying this inherited disorder would provide a window into molecular processes underlying the complex phenotype of speech development.

The inheritance pattern of DVD within the KE family suggested a monogenic autosomal dominant mode of transference. A genome wide study discovered a linkage in a region of chromosome 7 that co-segregated with the speech disorder, aptly named *SPCH1* [11]. A bioinformatic approach was used with existing BAC and PAC clones [12] to assemble, sequence, and further characterize *SPCH1* linkage information from the KE family to hone in on the critical interval responsible for DVD. Additionally, patients unrelated to the KE family but who were also diagnosed with DVD had translocations in *SPCH1*. This helped to identify an interval that mapped to the same BAC as a polyglutamate-repeat (poly-G) protein transcribed by the partially characterized *CAGH44* gene. Utilizing BAC clones adjacent to the *CAGH44* gene, a hypothetical sequence was determined and validated. Expanding the *CAGH44* gene, along with the poly-G portion, was a coding region with a high similarity to the DNA binding sequence of

the forkhead/winged-helix (FOX) family of transcription factors [13]. Thus, a mutation in the *FOXP2* gene was identified as the genetic basis of DVD [14].

FOXP2: An Orchestra Without a Maestro's Baton

The identification and characterization of the *FOXP2* gene led investigators to uncover its role at the molecular level. The *FOXP2* gene encodes the FOXP2 protein, a 715 amino acid Forkhead box family member containing the aforementioned DNA binding FOX domain [15], the poly-G region, and a zinc finger-leucine zipper domain involved in protein dimerization [16]. The hetero- and homodimerization of FOXP2 plays a crucial role that allows for the protein to bind to DNA via the forkhead/winged helix domain [17]. FOXP2 generally acts as a transcriptional repressor [18], binding to a sequence specific region [19-20] to regulate gene expression. In the KE family, a heterogenic guanine to adenine single nucleotide polymorphism causes a substitution of an arginine to histidine at amino acid 553 in the third helix of the DNA binding domain, disrupting FOXP2's ability to bind to DNA and influence gene expression.

This heterogenic mutation only manifests itself in speech development and production, even though FOXP2 is expressed in the lungs, cardiovascular tissue, gut, and brain. FOXP2 plays an important role in embryogenesis, and within the brain, FOXP2 is localized to the cortical plate, basal ganglia, thalamus, and cerebellum. The abnormal gray matter in the basal ganglia of affected KE family members points to the role FOXP2 plays in its development. The region-specific expression pattern suggests FOXP2 helps coordinates the development of motor related circuits [21]. In the case of the KE family, the mutation to the FOXP2 DNA helix diminishes its ability to coordinate gene expression, which may contribute to the developmental impairment of the motor related circuits driving the fine movements related to speech production.

Enter the Zebra Finch: A Songbird Model for Vocal Learning

At first glance, zebra finch (*T. guttata*) and humans have little in common; these songbirds sing and fly, whereas humans are ground bound and some sing better than others (most identify in the others camp). However, what humans share with the male orange-cheeked songbirds is vocal learning, making the zebra finch an experimental model system for mechanisms underlying learned vocal production [22]. Zebra finches and humans have similar critical periods for vocal learning. In finches, vocal learning begins with the sensory acquisition phase where a tutor song must be memorized, followed by a sensorimotor phase, where the juvenile practices the memorized song, modifying it over time until the song crystallizes at ~90d **(Fig. 1)** [23]. Additionally, vocal learners share similar neuronal connectivity facilitating vocal production, composed of a striatal-cortical-thalamic loop [24]. A molecular view of these shared vocal learning brain structures demonstrated similar gene expression patterns between the two species. Notably, the human basal ganglia shared similar gene expression with the songbird striatal nuclei Area X, a region that functions to facilitate and modify song output throughout the critical period [25]. The physiological and gene expression commonalities play a role in the development of vocalizations, and in both species, as does the localization of FOXP2 expression.

FoxP2 in the zebra finch brain plays a key role in vocal learning and vocal production throughout the songbird's lifespan. *In situ* hybridization studies of *FoxP2* mRNA in the zebra finch brain highlight its localization in the cortices, cerebellum, and striatum, all key areas for motor output [26]. In concordance with the basal ganglia abnormalities in DVD affected members of the KE family, FoxP2 expression in Area X is highly correlated to the quality of song production and learning. Perturbations to FoxP2 in Area X of juvenile male zebra finch, either by knockdown [27] or overexpression [28], produced impairments in song learning,

signifying that FoxP2 levels need to be properly regulated during this critical period. As the zebra finch moves from juvenile to adult, this continued regulation is necessary for song maintenance [29]. FoxP2 is both behaviorally and socially regulated. The song a male zebra finch produces is a marker for sexual selection by the females, as such, the male strives to produce the best quality of song when performing in front of a possible mate. This so-called 'directed' song has high stereotopy, and within Area X, FoxP2 levels remain at its baseline level [30]. During the male's song practice, where song variability is much higher, FoxP2 levels decrease [31]. The connection between the dynamic behavior of singing and regulation of FoxP2 expression demonstrates the close link between FoxP2 and vocal output.

Connecting Robust Gene Expression to a Complex Phenotype

By focusing in on FoxP2's role facilitating vocal learning, the gene expression forest may not be seen due this very important tree. Given FoxP2's function as a transcription factor and its dynamic regulation in behavioral settings, its expression can be tied to the regulation and expression of downstream genes. Studying complex phenotypes, whether disease related or behaviorally motivated, requires complex analytical tools to determine how genes work in concert with one another. Weighted gene coexpression analysis (WGCNA) was developed to determine how genes behave and group them together into functional modules based on shared mRNA expression patterns [32]. WGCNA on the striatal regions Area X and the adjacent VSP in the zebra finch demonstrated vastly different gene expression profiles and groups of genes correlated to the singing phenotype were identified within Area X, supporting the importance of Area X in song production. Additionally, some genes within the singing correlated modules were known FoxP2 regulated targets in humans [33-34]. FoxP2's relationship to vocal learning was explored similarly through WGCNA in juvenile zebra finch Area X cells. The gene network

obtained was correlated to the quality of learning by the juvenile, and modules identified were mined for possible links between song learning and song production. Comparing gene expression profiles between male juvenile and adult Area X showed gene network preservation between singing correlated genes, however the juvenile learning gene modules were poorly preserved in the adults [35]. These gene networks showed that gene expression is closely tied to the social development of the zebra finch, however, the pressing question remains how FoxP2 coordinates expression of these genes, providing a first step in many possible pathways.

FoxP2 Chromatin Immunoprecipitation

Chromatin immunoprecipitation (ChIP) is a technique utilized to capture protein-DNA interactions. A FOXP2 ChIP-microarray (ChIP-chip) using human brain regions, the inferior frontal cortex and basal ganglia, identified FoxP2 target genes, as well as regional differences between the two, providing evidence of differential FoxP2 targeted gene regulation [36]. A follow up ChIP-chip in cell culture and mouse embryonic brain demonstrated biological processes of identified FoxP2 target genes, showing enrichment in locomotory behavior, axon guidance processes, and ion transporter activity [37]. As the brain develops, FoxP2 targets genes that function for neuronal growth, possibly increasing connectivity between key motor brain areas [38]. The identified processes provide further evidence in FoxP2's role in coordinating gene expression necessary for neuronal activity connected to motor output.

These fundamental studies began to unravel FoxP2 target genes, but how the dynamic regulation of FoxP2, and its subsequent effect on gene expression, contribute to vocalizations remains unanswered. Developing a FoxP2 ChIP experiment in active vocal learning zebra finch would provide evidence of FoxP2 regulating specific genes correlated to song learning from juvenile regulating the genes correlated to song learning from the WGCNA data set.

Additionally, by validating the ChIP through quantitative PCR, the next logical step is to use next generation sequencing (ChIP-seq) to identify FoxP2 targets throughout the genome. This unbiased approach can be applied to multiple stages of development, juvenile and adult, as well as identify FoxP2 target differences within the singing phenotype by comparing the sexual differences between male and female. The following thesis provides a detailed description of a FoxP2 ChIP for specific genes for validation, as well as FoxP2 ChIP-seq, both novel in the zebra finch model, to begin to determine how FoxP2 orchestrates gene expression tied to vocalizations as well as song learning.

Figure 1. Vocal learning timelines between humans and zebra finch

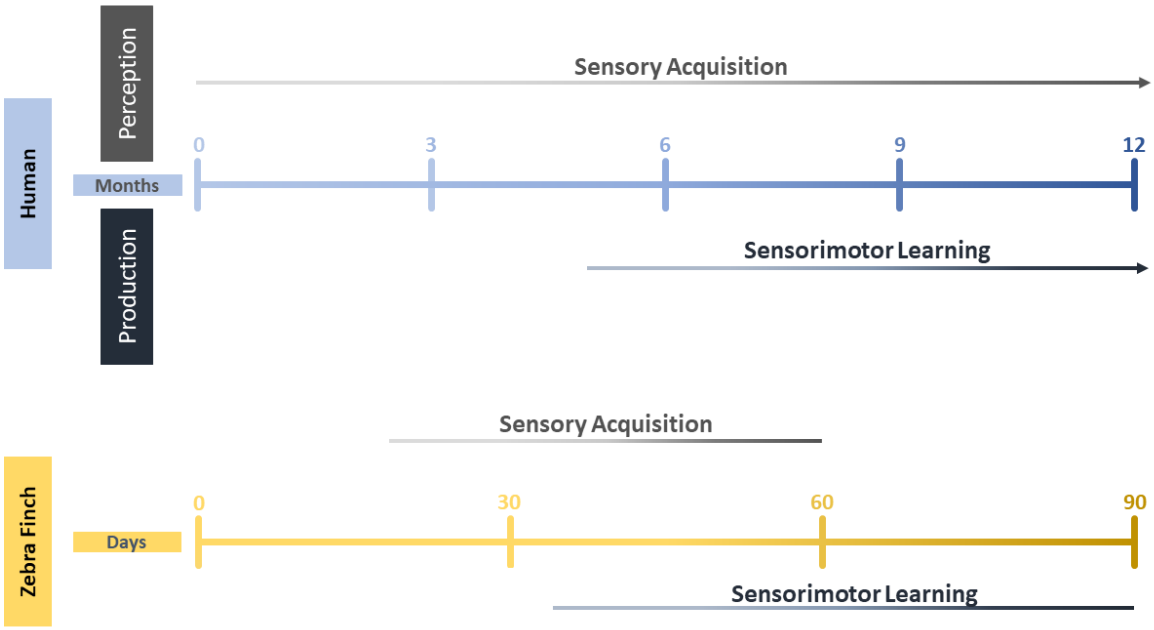

The developmental timelines of human speech and zebra finch song begin with the sensory acquisition phase. The juveniles listen to adult vocalizations to form a neural template of these sounds. Following the beginning of the sensory acquisition phase, both species begin the process of sensorimotor learning, where the juvenile makes the learned vocalizations and begins to modify these sounds to better match the learned template. In the zebra finch, the song crystalizes upon adulthood and is permanent, whereas humans are capable of adding to their vocalization throughout life. Figure is adapted from Doupe and Kuhl, 1999.

Methods

Subjects

All animal use was in accordance with NIH guidelines for experiments involving vertebrate animals and approved by the University of California, Los Angeles Chancellor's Institutional Animal Care and Use Committee. Adult subjects older than 120d post hatch (dph) were selected from our aviary for the ChIP validation and qPCR experiments. Juvenile male birds were isolated from their home cage at 35 dph and remained until 65 dph. On their 65th dph, they were selected for either non-singing (NS) or singing group (S). The NS group was obtained by the experimenter sitting near to the bird's cage in the morning and, if the bird attempted to sing, gently distracting it from singing for two hours after lights-on. Birds who never-the-less sang 10 or more motifs were not used on that day. Those that sang less than 10 motifs in the first two hours were then left undisturbed for an additional hour and then sacrificed. This methodology previously resulted in gene expression profiles that were similar to those of birds that do not sing of their own volition (Hilliard et al., 2012), suggesting that it does not induce a sizeable stress response. To be included in the group, birds must have sung > 90 motifs during the same 2-hour window. Those that met these criteria were sacrificed 1 hour later. The subjects were sacrificed by rapid decapitation and brains were extracted and frozen by liquid nitrogen.

Chromatin Immunoprecipitation

Chromatin immunoprecipitation (ChIP) was performed using ChIP-IT High Sensitivity (Active Motif, Cat. No. 53040) following manufacturer's protocol. Whole brain was isolated from an adult male zebra finch, minced, and crosslinked in a formaldehyde solution. The tissue was homogenized with a hand-held tissue homogenizer for 45 s at 35,000 rpm. Following homogenization, the sample was sonicated at 25% amplitude, 30 s on, 30 s off, for 30 minutes.

portion of the sonicate was de-crosslinked and quantified by a Nanodrop 1000 (Thermo Scientific, F713). The sample was split evenly into three tubes. A cocktail of 4 µg of anti-FoxP2 primary antibodies were applied to one sample (Thermo Fisher, Cat. No. 720031, Abcam, Cat. No. ab1307, and Santa Cruz, Cat. No. sc-517261), IgG in another (Millipore, Cat. No. 12-370), and the third used as input DNA. After an overnight incubation, the samples were washed, decrosslinked, and subjected to further PCR analysis.

PCR and Quantitative PCR

The promoter region of *MAPK11*, determined to be 100 bp upstream of the transcription start site (TSS) was identified by searching in the NCBI database the transcript ID. Primers to this region were manually binned into 100 bp regions. The *MAPK11* primers were as follows: forward 5'-CCCTTTCCCCAAATGGCAGA-3' and reverse 5'-TATGAGCCTTGCCTTGGAG C-3'. The initial PCR experiment was performed using DreamTaq PCR Master Mix per manufacturer's protocol. A PCR protocol was used as follows: (1) 95° C 1 min, (2) 95° C 30 s, (3) 67° C 30 s, (4) 72° C 1 min, repeat (2-4) for 40 cycles, (5) 72° C 10 min. PCR product was run on a 1.5% agarose gel in presence of SYBR Safe to allow for visualization of DNA. PCR products were purified (QIAQuick Gel Extraction Kit) and sent for sequencing by Laragen, Inc. Reverse primers sent for sequencing are as follows: 5'-TATGAGCCTTGCCTTGGAGC-3' and 5'-CCTATGAGCCTTGCCTTGGA-3'.

Quantitative PCR was performed on the Thermo Fisher QuantStudio 3. PCR was performed using PowerUP SYBR Green Master Mix (TermoFisher Scientific) with the following conditions: (1) 50° C 2 min, (2) 95° C 2 min, (3) 95° C 15 s, (4) 60° C 15 s, (5) 72° C 1 min, repeat (3-5) for 40 cycles. All reactions were run in triplicate for FoxP2 ChIP, IgG, and input samples. Primer region amplification was quantified and FoxP2 ChIP and IgG was normalized to

input using 2-Δ ΔCT method [39]. The following primer sets were constructed similarly to *MAPK11*: *ACTB* (Beta-Actin) and 1000-3000 bp upstream from *CNTNAP2* TSS for negative controls and the promoter region of *CNTNAP2* for a positive control. All primer constructs used are annotated in Table 1.

MAPK11 Expression and Western Blot Following FoxP2 Overexpression

FoxP2 overexpression was achieved by bilateral injections of FoxP2-AAV detailed previously [34]. Area X was punched and subjected to either RNA isolation by Qiagen RNeasy Plus Kit (Cat. No. 74134) or protein isolation via homogenization in RIPA buffer. Western blot was performed on a 12% poly-acrylamide gel with MapK11 primary antibody (Cell Signaling, Cat. No. 9212S, 1:1000 dilution). MAPK11 RT-PCR primers for RNA expression are located in Table 2. RNA extracts were reverse transcribed using iScript cDNA Synthesis Kit (Bio-Rad, Cat. No. 170-8891) per kit instructions. qRT-PCR was performed as detailed above.

Next Generation Sequencing Library Preparation

Input and FoxP2 ChIP samples were quantified (Qubit 1.0 Fluorometer) and diluted to 0.5 ng. Library preparation was performed using NuGen Ovation Ultralow Library System V2-32 (Cat. No. 0344-32) per manufacturer's instructions. Briefly, ChIP samples were end repaired and sequence specific adapters were ligated to each sample. Following ligation, the DNA fragments were magnetic bead purified and PCR amplified with the following conditions: (1) 72° C 2 min, (2) 95° C 3 min, (3) 98° C 20 s, (4) 65° C 30 s, (5) 72° C 30 sec, repeat (3-5) for 15 cycles. The amplified DNA was subjected to a final round of bead purification.

Next Generation Sequencing

Library preparations were quality assessed by the Agilent 4200 TapeStation system (Cat. No. G2991AA) using D1000 Screen Tape. The ChIP libraries were quantified by the Qubit 1.0

Fluorometer and diluted to 10 nM, Libraries from each sample were combined and sequenced across two lanes by the UCLA Neurogenomics Core (UNGC; https://www.semel.ucla.edu/ungc) by the Illumina HiSeq 4000 sequencer, generating between 15 and 50 million 65 bp single-end reads per library. Reads were demultiplexed by UNGC and shared with us via file transfer protocol.

ChIP-seq Preprocessing and Data Analysis

Raw single-end FASTQ files provided by UNGC underwent quality control analysis by FastQC (bioinformatics.babraham.ac.uk/projects/fastqc), indicating good sequencing quality, with high confidence base calling across all bases in each sample with no adapter contamination. There were 3 biological replicates and an input control sample per group. Raw reads were aligned to the Ensembl zebra finch genome assembly 3.2.4 (release 92) using Bowtie2 [40] with default parameters and a Bowtie2 index built using bowtie2-build. SAM alignments were converted to BAM and sorted using Samtools [41]. Peak calling was performed using MACS version 2.1.1.20160309 [42], using input sequencing as a control (input sequencing was performed for each biological group), with the following parameters: --down-sample --seed 123, -g 1.2e9. All peaks called for a biological replicate were combined with peaks of all replicates within the same group using the union() function within the GenomicRanges package [43] in Bioconductor [44]. We identified peaks within promoter regions (defined as 2000 bp upstream and 200 bp downstream from the TSS) of genes (from Ensembl database, release 92). Due to the sparse annotation of the zebra finch genome, Ensembl gene IDs were matched to human paralogs from the HUGO Gene Nomenclature Committee (HGNC) [45], RefSeq [46], and NCBI databases using BiomaRt [47]. Genes with HGNC paralogs were piped into a custom KEGG pathway analysis that uses KEGG.db [48], a Bioconductor package. ChIPseeker [49] was used to

generate average profile plots of peak occupancy over all TSSs. Additionally, FoxP2 consensus binding motif, downloaded from the JASPAR database [50] and converted into a position-weight matrix (PWM), was used with the Biostrings package [51] (from Bioconductor) to identify regions of the genome that match the FoxP2 motif with 80% confidence, and distance to motif was calculated using the distanceToNearest() function from the GenomicRanges package. Genome browser tracks (bigWig files) were generated using the bamCoverage function within deepTools [52] version 3.0.2, and visualized using the Integrated Genome Browser [53] (bioviz.org). *ATF4*, *RPL12*, *RPL22*, *RPL29*, and *RPL34* qPCR for ChIP-seq validation was performed as detailed above (Primer sequences can be found in Table 2).

Table 1. Primer Sequences for ChIP-qPCR

Gene	Start	End	Forward 5'-3’	Reverse 5'-3'
MapK11	483	321	GCTCCAAGGCAAGGCTCATA	CCAGTCTGGGGACATTATGGT
	342	232	GTCCAGGACTTATCCCCAGG	CCTATGAGCCTTGCCTTGGA
	253	141	GCAGCCAGGGAACTAGTCAG	TGCCTGGGGATAAGTCCTGG
	208	108	CCTTTACCCTCTTGCACCTTCT	GCTAGATGGAAAACAAGGCACC
	161	92	AGGGCTCTTACCCCTTCCTT	GCTGACTAGTTCCCTGGCTG
CNTNAP2	997	899	TGAAGTGGTTAAGACCGTGTGT	TAGGCACTGTACTCCCTCGG
	898	810	TTAGAGGAGCCCCAAAGCAG	TCACAGTCACTAAATAACAGCAGGT
	77	2	GCAATAACCTCCCAGCTCAGATA	TGTGAGTGCGTGTTTGGCT
CNTNAP2	1551	1834	CTTCTGTTCCTCTCCTGCTGT	TGGTCTGCTGAGCCTTTAAGT
Negative	2113	2334	AGATTCAGCAGGCTGGTTGG	GCAGGCCTCACTTGTGGTTA
ACTB	888	817	CACAATGCCACATGCAAGGA	ATCGTGCACACCAGTGTAGG
	674	549	GTGCAACATGCAGATCGGTG	TGTGGGATGCTGATGCATGT

Table 2. Primer Sequences for RNA Expression via qRT-PCR

Gene	Forward 5'-3’	Reverse 5'-3'
MapK11	GGAATCATCCATCGGGACCT	GGATTGGCACCACGAAACAC
ATF4	CGGGAGTACCCCACCAATTC	CTCCTGTTCCGCCCTCTTTT
RPL12	ACAGGCAAGCGCAGATAGAG	GGGTGTCTCCCATCAATGCT
RPL22	ATCGAGAGGAGCAAGAGCAAG	GATCTGGAAGTAGCGCAGCTC
RPL29	GCACAACCAGTCCCGTAAGT	TCAGCCCCTTCTTGTTGTGT
RPL34	GGCGCCAGGGGTGAAA	TCCTGTCACGGACACACTTG

Results

Foxp2-ChIrP: Optimizing a ChIP Protocol to Investigate Song Learning Pathways

WGCNA is a valuable tool to organize genes into distinct modules based on shared expression values [31]. To untangle this web of interconnected genes, further bioinformatic approaches led to the identification of modules and individual genes correlated to the quantifiable song learning phenotype [34]. This analysis identified *MAPK11* as the gene with the greatest gene significance to learning. Although not a member of the module with the overall highest correlation to learning, *MAPK11* was highly connected to its members. With the hypothesis that *MAPK11* plays a role in vocal development, and the knowledge of FoxP2 as a vital transcription factor underlying vocal learning, the next question is whether FoxP2 targets *MAPK11* to influence gene expression.

FoxP2 Chromatin immunoprecipitation (ChIP) has been examined in mice and humans, but not in the zebra finch model. I therefore had to develop an optimized protocol which is presented here as part of the results section. The ChIP process necessitates the extraction of enough chromatin as starting material with which to begin the protocol. Isolation of chromatin specifically from the song dedicated nuclei would be insufficient for the amount of starting DNA needed, thus, the entire telencephalon was utilized. Following the cross-linking of DNA-protein interactions with formaldehyde, DNA sonication, the breaking of the DNA into sizable fragments for subsequent pulldown, was optimized to achieve fragments between 200-1000 bps in length (**Fig. 2A)**. The most important aspect of a ChIP involves the antibody selection for FoxP2 pulldown. Throughout the ChIP protocol, FoxP2 remains in its native conformation, thus an antibody must recognize an available epitope. As a way to hedge our bet, three antibodies were chosen to target different regions of the FoxP2 protein (**Fig. 2B**). FoxP2-specific pulldown

validation was achieved by PCR for genes that have been previously shown to contain FoxP2 target regions (i.e. positive controls) and genes/regions void of FoxP2 binding (negative controls). *CNTNAP2* is a direct target of FoxP2 in zebra finch [54] and was used as a positive control (**Fig 2C)**. As negative controls, previous FoxP2 ChIP-chip studies utilized β-actin (*ACTB*) as a region free of FoxP2 binding, and as a more specific negative control, a region 3000-2000 bp upstream from the *CNTNAP2* transcription start site (TSS), deemed CNTNeg, was selected (**Fig 2D)**. Following DNA pulldown and purification, PCR demonstrated enriched pulldown of *CNTNAP2* positive control regions and void of enrichment at the negative controls when compared to non-specific IgG (**Fig 2E**).

Confirming MAPK11 as a FoxP2 Target via ChIP-qPCR

Following FoxP2 ChIP-qPCR validation, novel targets of FoxP2 could now be investigated. Using the JASPAR database, a resource for transcription factor binding sequences, the FoxP2 binding motif was transformed into a position weight matrix (PWM). I then searched through the *T. guttata* genome for genes whose promoters matched the matrix with a confidence interval of 0.80 (**Fig. 3A**). Fortuitously, the gene with the greatest significance to song learning, *MAPK11* contained a 10 bp motif within its promoter region with a one bp difference to the canonical FoxP2 binding motif. Primers were designed (**Fig. 3B**) and qPCR on FoxP2 ChIP samples showed an enrichment of DNA pulled down from these regions compared to IgG, providing evidence that FoxP2 binds to the promoter region of *MAPK11* containing the FoxP2 binding motif (**Fig. 3C**). Ensuring the PCR product was in fact our region of interest, the amplified product was verified by sequencing (**Fig. 4**).

FoxP2 bound to the promoter of *MAPK11* tells one aspect of this interaction, but the question of regulation remains. A viral construct to overexpress FoxP2 was injected into Area X

of juvenile males according to our RNA-seq protocol [34]. Bilateral punches were retrieved, one set up for RNA extraction, the other for protein extraction. Surprisingly, the increase in FoxP2 expression did not significantly affect *MAPK11* expression RT-qPCR (**Fig. 4A**) nor were changes in protein quantity via Western blot analysis (**Fig. 4B**). Our inability to detect changes in *MAPK11* qRT-PCR signals following FoxP2 over-expression could reflect *MAPK11*'s enormous number of roles in various biological pathways, signaling cascades, and its overall importance to cell function.

Identifying Differential FoxP2 Binding Sites by ChIP-seq

The ChIP-qPCR experiments demonstrated FoxP2 binding to the promoter region of *MAPK11*, however, to say this is the tip of the iceberg does a disservice to tips of icebergs. The importance of FoxP2 to learned vocalizations has been demonstrated multiple times in both humans and songbirds, with its dynamic expression driving further gene expression changes throughout this complex phenotype. Following up the initial ChIP work, ChIP-seq across different sexual and groups would shed light on how FoxP2 differentially targets genes. In order to capture sex differences, adult male and adult female zebra finches (n=3) were selected, and for developmental differences, male juveniles (65 dph) were chosen for ChIP-seq. Additionally, the juveniles were split to have a non-singing (NS, n=3) and a singing (S, n=3) group, knowing that FoxP2 expression changes specifically within Area X with this behavioral paradigm [26]. We hoped to find genes where FoxP2 was bound that highlight the differences in the singing phenotype (M v F and Juv NS v S) and the learning phenotype (M v Juv).

Sequencing libraries were prepared from the isolated ChIP DNA with specific adapter barcodes, validated for fragment length and quality, diluted to 10 µM, pooled together into 2 lanes, and supplied to the UNGC to sequence and de-multiplex. The quality of sequencing was

checked and validated via FastQC (**Fig. 6)**, showing high confidence of each base sequenced. Sequenced reads were aligned to the *T. guttata* genome, downsampled to the lowest aligned read count, and input DNA controlled before peak calling (**Table 2**). Peak width was determined to ensure small peak ranges (**Fig 7A)**. If the ChIP protocol was successful, the proximity of the peaks to the JASPAR defined FoxP2 motif would be close. By using a threshold of 0.80 sequence match, the distance of the location of each peak to a motif was determined, validating the pulldown was specific to FoxP2 binding sites (**Fig. 7B**). Further validation of peak location was achieved by determining the peak frequency around the promoter TSS (**Fig. 7C**), with each group showing higher peak frequency near the TSS. In summary, validation of proper FoxP2 ChIP pulldown was demonstrated by the peaks of each group having uniform width, located in close proximity to a FoxP2 binding motif, and a higher peak frequency relative to TSS.

Identifying FoxP2 binding sites within the promoter region gave a number of genes for comparison (**Table 3**). Applying HNGC gene symbols to the Ensemble gene IDs diminished the list of genes with known functions within the zebra finch genome considerably, due in part to its incomplete annotation. Nevertheless, the analysis persists. KEGG pathway analysis determined key contributors to biological function both within each group and between the group comparisons. The KEGG analysis on total genes, regardless of group, with FoxP2 bound to the promoter highlighted two pathways worth further exploration: ribosomal and neurotrophin signaling pathways. Interestingly, when comparing the male and female FoxP2 binding sites, both ribosomal and neurotrophin pathways are observed in only the male. In the adult male and juvenile, only the adult continues to have the ribosomal pathway present. The neuotrophin pathway was a key KEGG pathway difference between the juvenile S and NS, with the juvenile singer having FoxP2 bound to key genes within this pathway (**Fig. 8**). This observation led to the

hypothesis that these genes play a role in the singing phenotype, and engaged in a process that is age dependent. In the adult male, the ribosomal genes *RPL12*, *RPL22*, *RPL29*, and *RPL34*, were all observed having FoxP2 binding, which was not seen in any other group, possibly, an age and sex related difference in processing of RNA. Within the juvenile, singing leads to a decreased level of FoxP2 expression in Area X, which may activate the neurotrophin pathway, specifically by FoxP2 binding to the promoter region of Activating Transcription factor 4 (*ATF4*) promoter region. ATF4 is a transcription factor observed as a regulator of $GABA_B$ receptor trafficking, a key component to synapse plasticity and memory formation [55] (**Fig. 9A**).

Building the connection of FoxP2 binding to these differential genes, qRT-PCR was conducted on adult male and female zebra finch, as well as a Juvenile NS. Unfortunately, due to the uncooperative manner of the juvenile songbirds, a Juvenile S was not available for gene expression analysis. Regardless, in the samples tested, the male zebra finch showed increased expression pattern for all genes (*ATF4*, *RPL12*, *RPL22*, *RPL29*, *RPL34*) shown to be bound in the adult male and not in females or juvenile NS (**Fig. 9B**). To further the link, the gene expression of profile of the female and juvenile NS showed remarkable similarity. This analysis was conducted with an n=1 in each group, so further testing remains to be done. Additionally, to further this claim, a juvenile S sample would be necessary to test if *ATF4* expression is similarly high, since it shares a FoxP2 binding site with the adult male, and if the ribosomal genes are low, as with the female and juvenile NS.

Figure 2. FoxP2-ChIP Validation

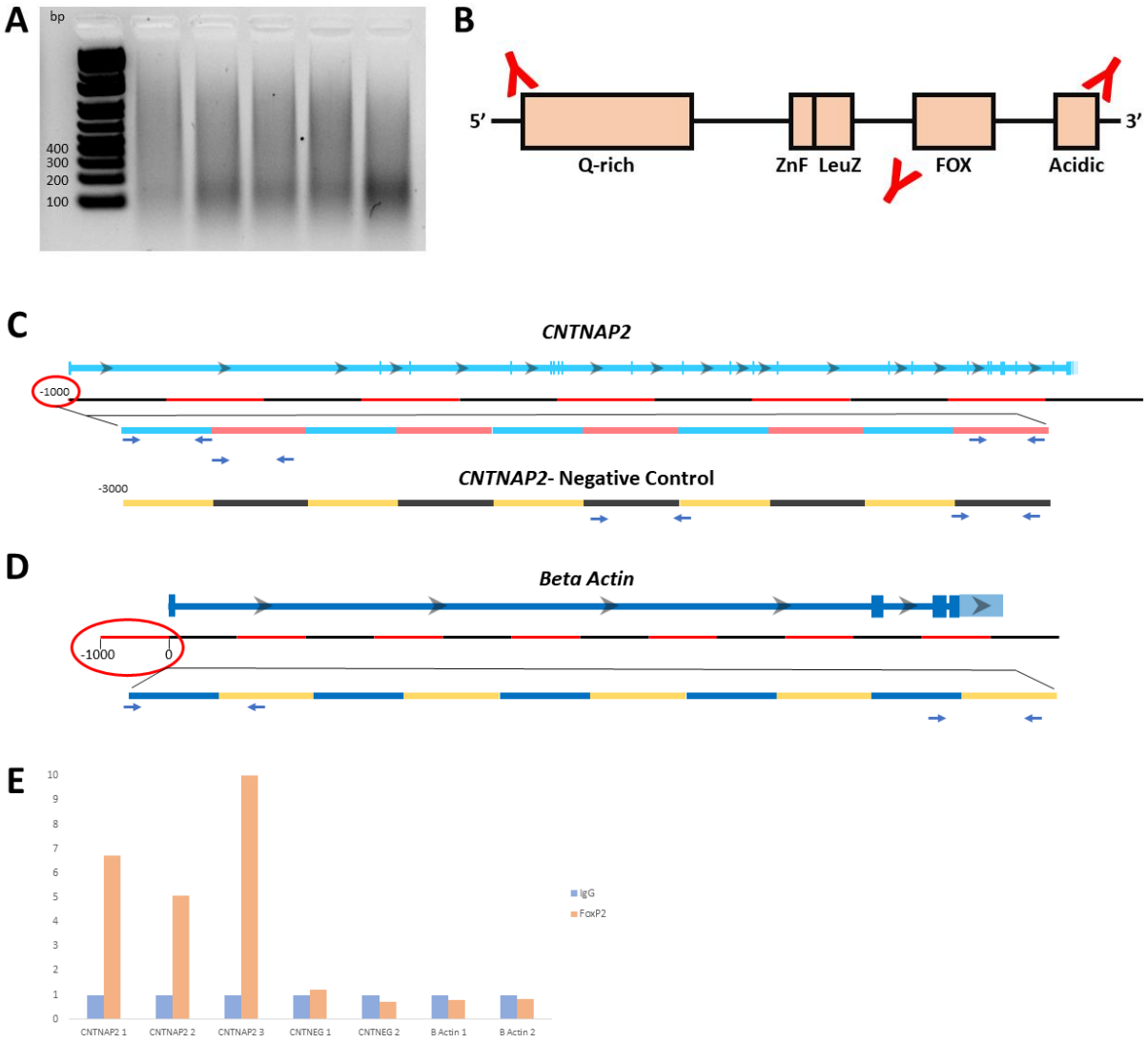

Figure 2. **A**) Sonication of DNA isolated from the zebra finch telencephalon with enrichment of fragments between 200-1000 bp. 1.5% Agarose gel stained with SyberSafe. **B)** Schematic of FoxP2 protein, red antibodies used to target different regions of the FoxP2 protein. **C)** *CNTNAP2* gene (teal) with highlighted promoter region and -3000- -2000 bps upstream below. Arrows signify primers for regions of PCR amplification. **D)** Negative control β-actin with promoter region and arrows for primers for PCR amplification. **E)** ChIP-qPCR results showing enrichment

of amplification from *CNTNAP2* positive control regions and negative results from *CNTNeg* and β-actin when normalized to non-specific IgG.

Figure 3. FoxP2 Binds to *MAPK11* Via Sequence Specific Binding Motif

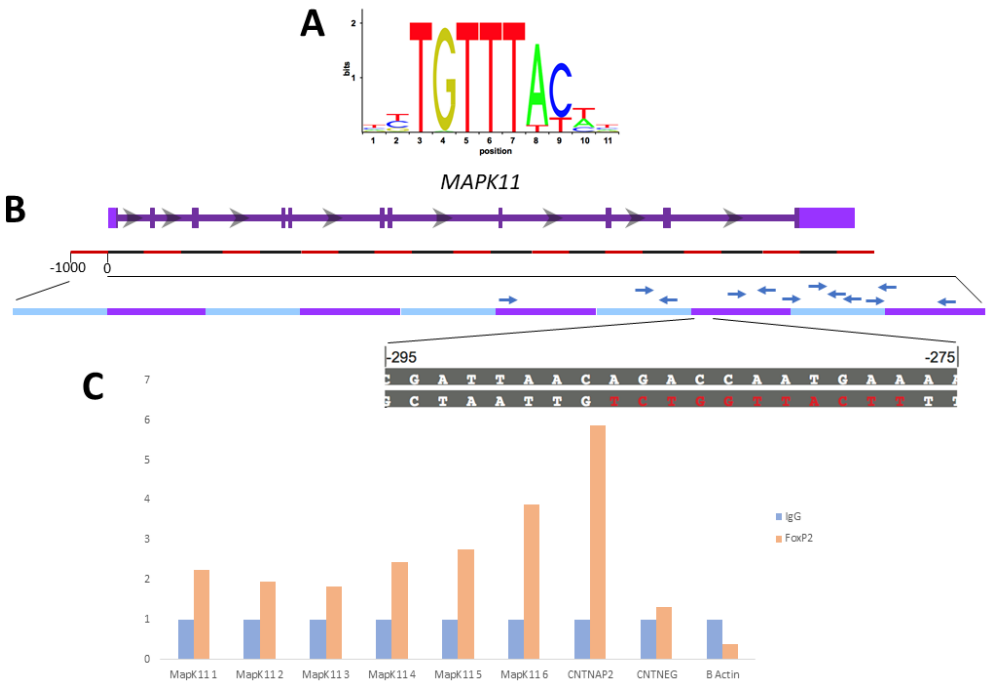

Figure 3. **A)** JASPAR database FoxP2 binding sequence, which was converted into a PWM and searched throughout the T. guttata genome promoter regions. **B)** Schematic of *MAPK11*, promoter region in teal and purple, blue arrows represent primers for regions of PCR amplification. Highlighted box below (-295- -275) represents sequence match for FoxP2 binding motif. **C)** FoxP2 ChIP-qPCR results for regions highlighted above. Overall enrichment of pulled down DNA from the *MapK11* primers compared to IgG with CNTNAP2 as the positive control and CNTNeg and β-actin as negative control

Figure 4. Sequence of PCR Amplified *MAPK11* Promoter Region

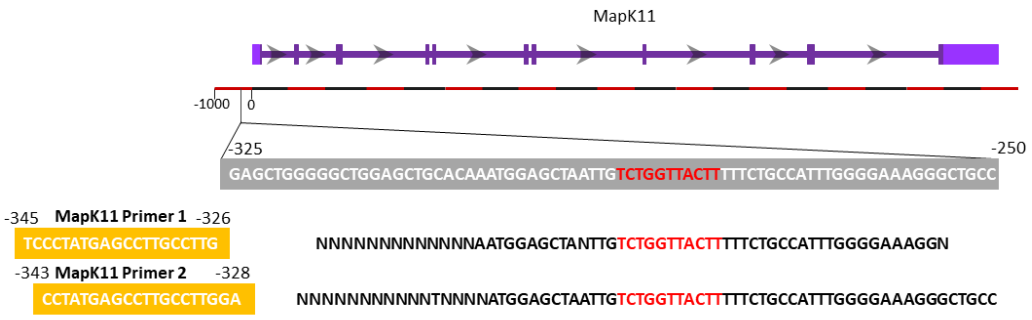

Figure 4. *MAPK11* schematic with highlighted regions targeted for ChIP-qPCR. PCR product was isolated and sent for sequencing with the primers in yellow. Sequencing results in black with red region signifying FoxP2 binding motif match.

Figure 5. FoxP2 Does Not Regulate of *MAPK11 Expression*

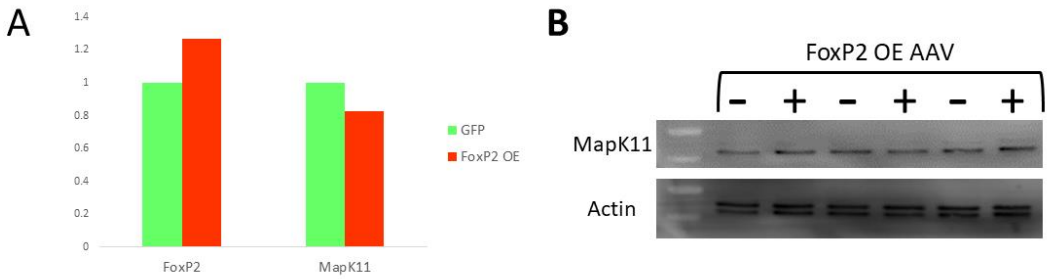

Figure 5. **A)** RT-qPCR on FoxP2 from Area X punches in which one hemisphere was injected with an AAV to drive FoxP2 over-expression. While an increase in FoxP2 is observed, no significant differences in *MAPK11* RNA expression was detected relative to the uninjected hemisphere. **B)** Western blot analysis shows no difference in MapK11 protein quantification following FoxP2 OE.

Figure 6. FoxP2 ChIP-seq Base Confidence via FastQC

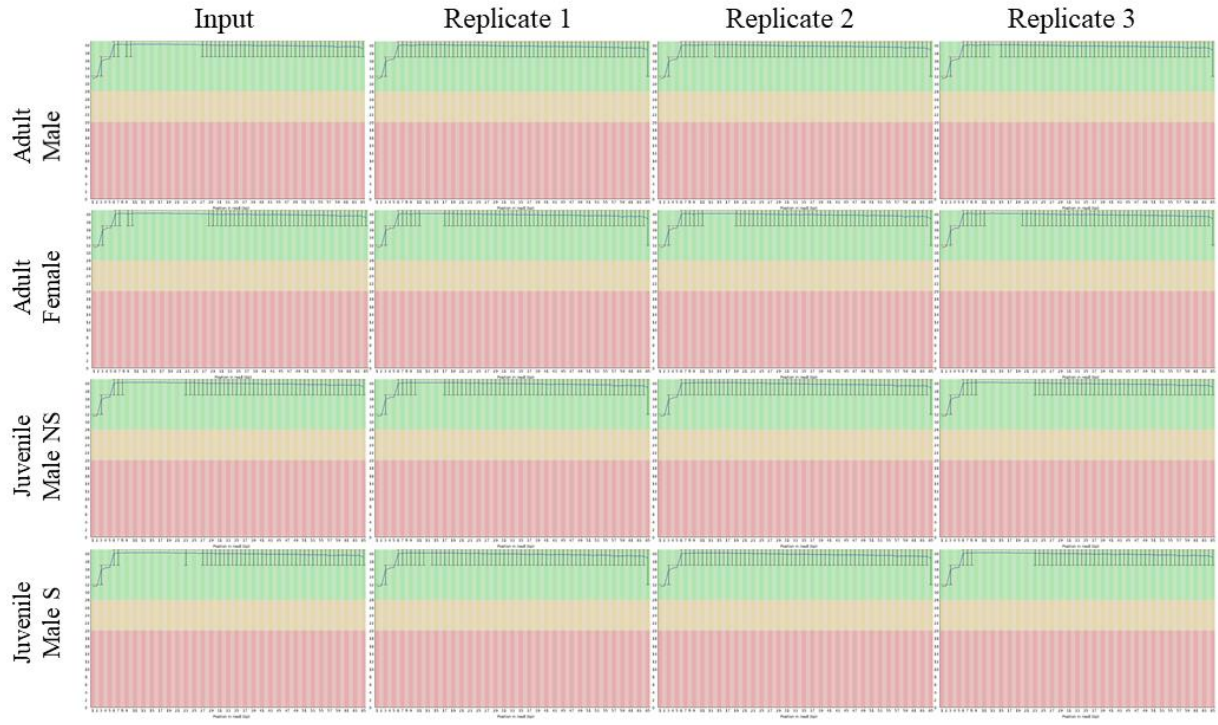

Figure 6. FastQC results for each sequenced sample. Each row is a single base and row is the confidence score. Green indicates high confidence in base calling. For each sample, the black trace falls within the green region.

Table 3. Aligned Reads and Peaks in Sequenced Samples

	Reads	Aligned Reads	% Mapped Reads	Number of Peaks
Adult F Input	52682934	45702287	86.75	5282
Adult F Average	29135155	24375707	83.66	
Adult M Input	49408845	43559577	88.16	5335
Adult M Average	18762813	15816448	84.30	
Juvenile M NS Input	71618720	63317203	88.41	4027
Juvenile M NS Average	28732780	24899762	86.66	
Juvenile M S Input	52903079	46292072	87.5	2688
Juvenile M S Average	21374580	18595482	87.0	

Table 3. Number of reads, aligned reads, % mapped and number of peaks for each group. The Average of each group was calculated from an n=3. Aligned reads were downsampled to Adult M Average aligned reads prior to peak calling.

Figure 7. FoxP2 ChIP-seq Peak Characteristics and Localization

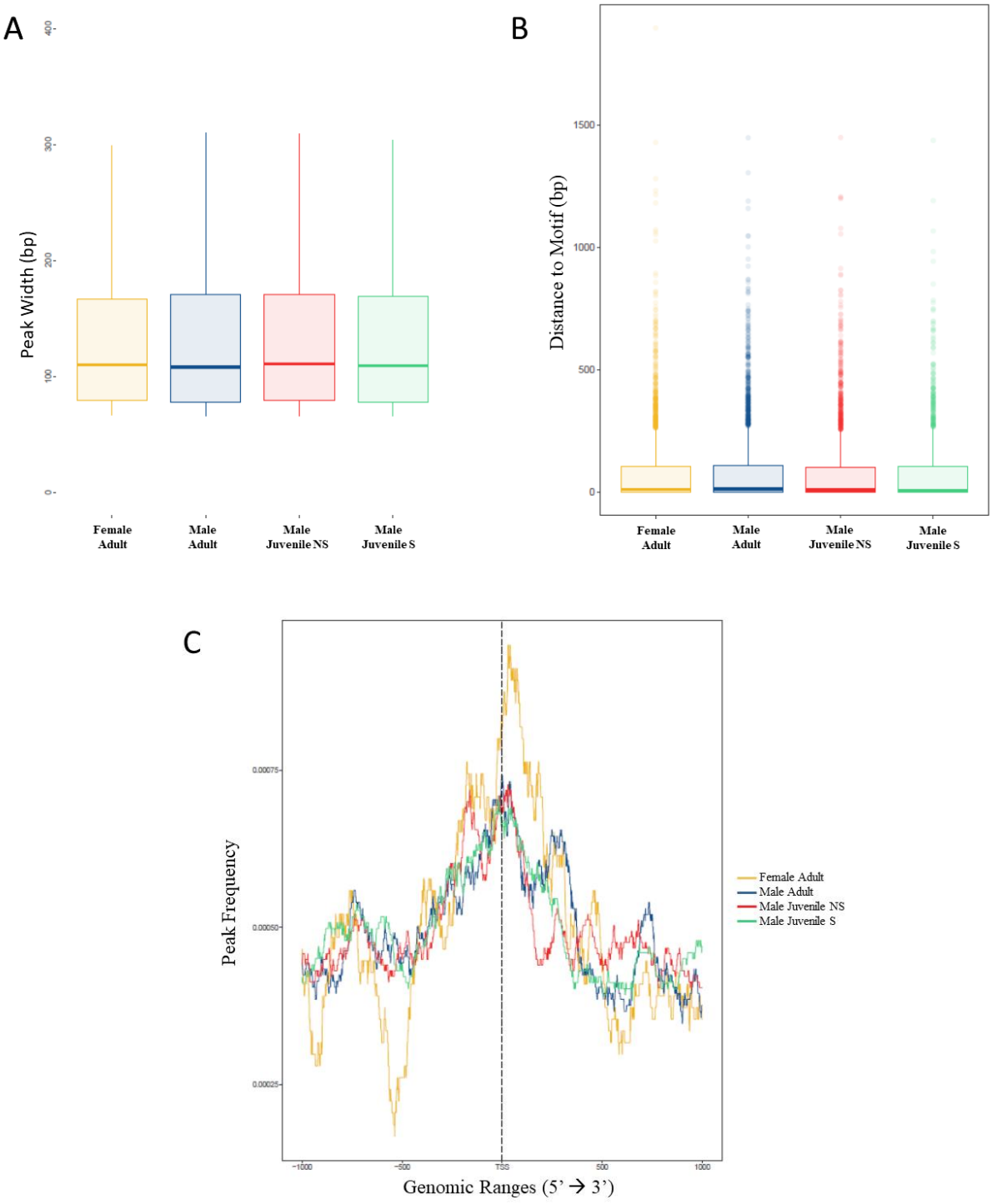

Figure 7. **A)** Peak width of each ChIP-seq group, average peak width ~110 bp **B)** Distance of each peak to the JASPAR database consensus FoxP2 binding motif, with a confidence of 0.80

match to the PWM. **C)** Peak frequency around the promoter region. The TSS is demonstrated by the dashed line, showing an enrichment of peak frequency at the TSS.

Table 4. FoxP2 Binding Sites Within the Promoter Region

	# of Genes	Genes with HGNC
Total *T. guttata* Genome	18585	10794
Bound in at Least One Group	475	279
Bound in All	89	15
Adult Comparisons		
Male and Female	123	33
Male	177	116
Female	83	47
Male Adult - Juvenile Comparisons		
Male and Juvenile NS	148	41
Male	152	108
Juvenile NS	59	43
Male and Juvenile S	135	39
Male	165	110
Juvenile S	60	46
Male Juvenile Comparisons		
Juvenile NS and Juvenile S	134	41
Juvenile NS	73	43
Juvenile S	61	44

Table 4. Number of genes observed with a FoxP2 binding site within the promoter region. The identified genes were given an ENSEMBL ID which was matched to HGNC genes, showing the total number of genes with known functions on the right.

Figure 8. KEGG Pathway Analysis of FoxP2 Differentially Bound Genes

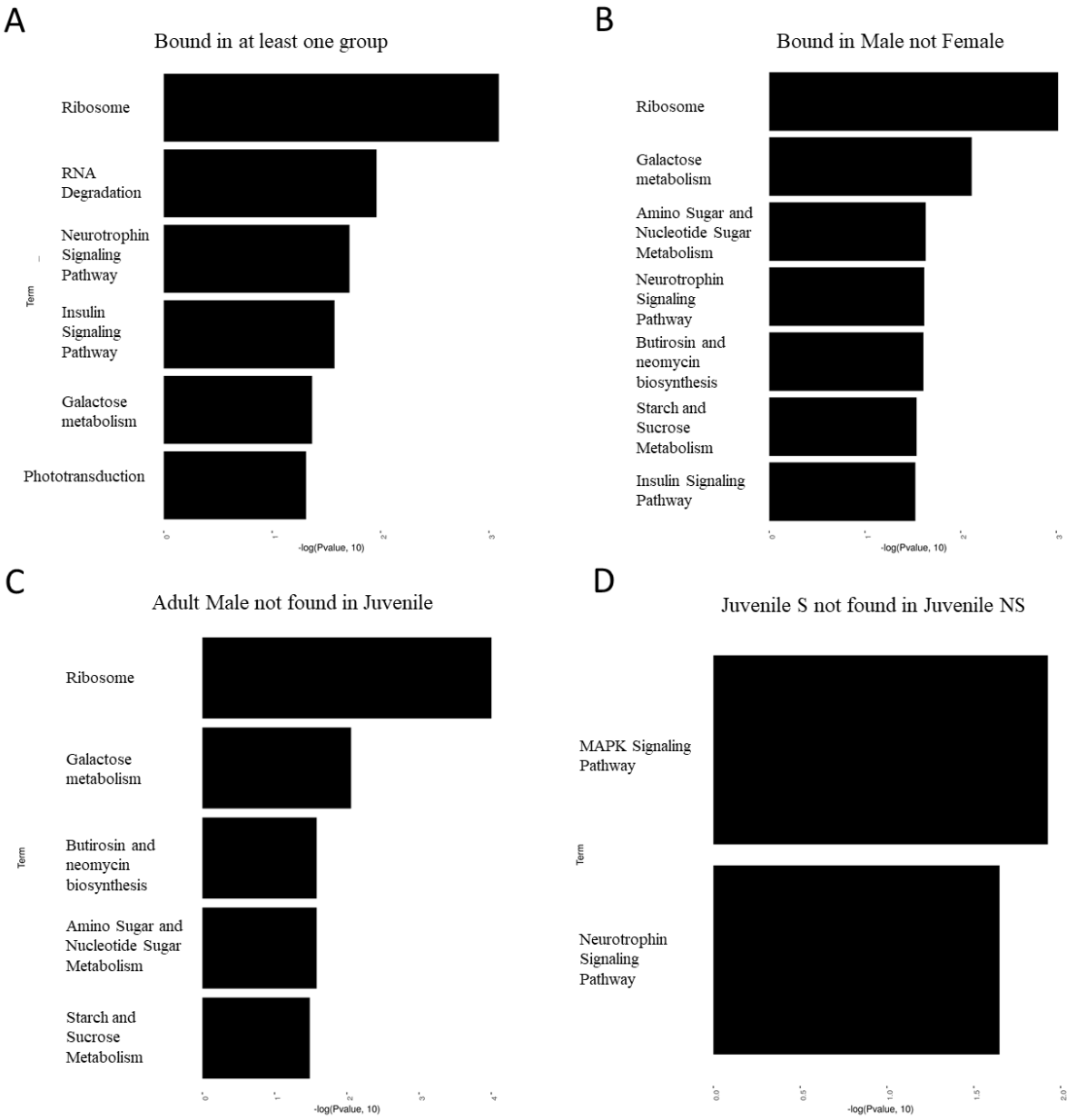

Figure 8. KEGG pathway analysis. **A)** Significant enriched terms within KEGG pathways of all gene promoter regions bound by FoxP2 throughout the groups. **B-D)** Comparison analysis of KEGG pathways **B.** Binding sites in males not found in females, **C.** Genes enriched in pathways found in adult males but not in male juveniles, **D.** Enriched pathways found in juvenile singers but not in juvenile non-singers.

Figure 9. Differential FoxP2 Binding Affects Gene Expression

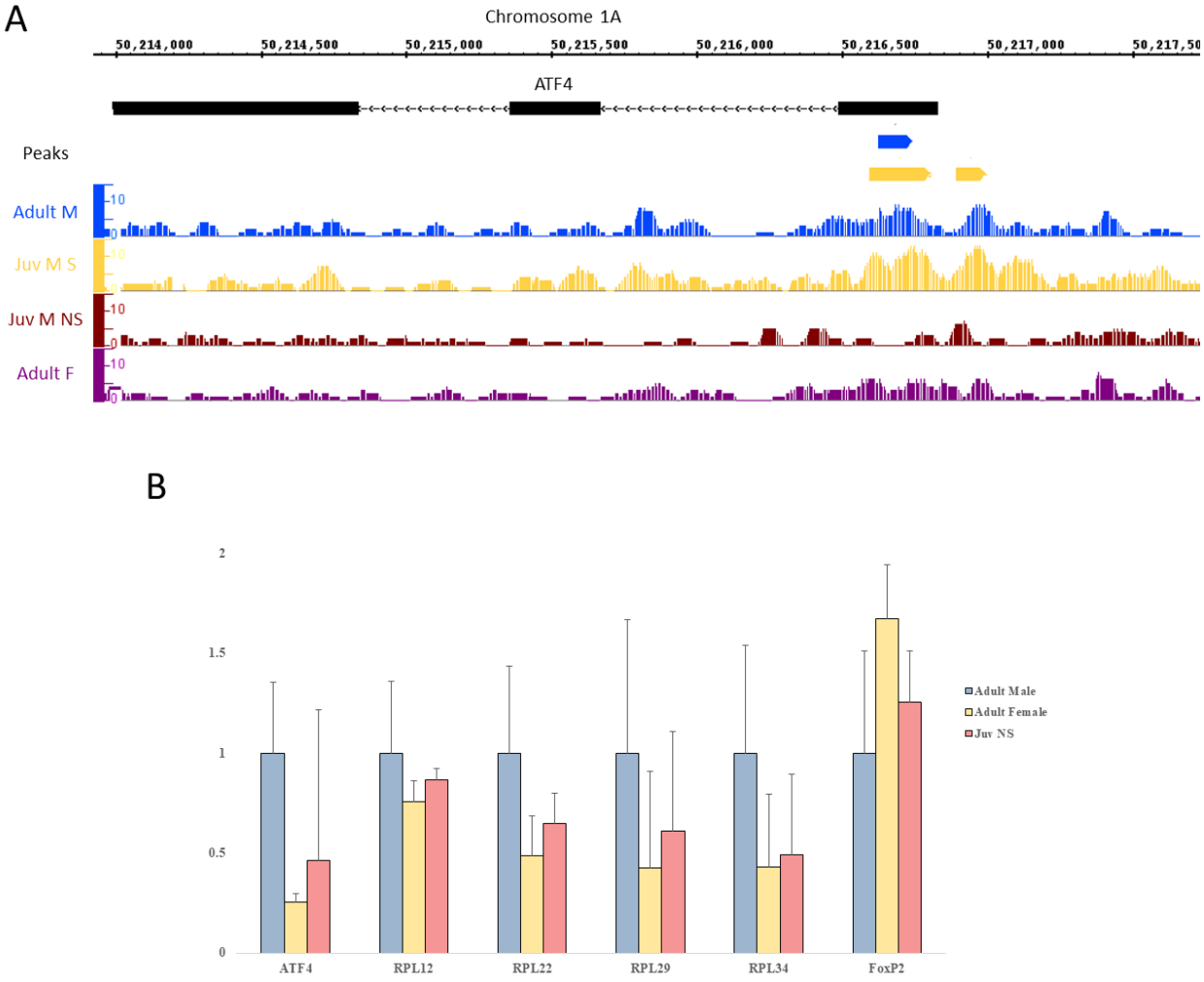

Figure 9. **A)** Peak visualization of the promoter region of *ATF4*. Chromosome 1A schematic with *ATF4* coordinates top. Peaks labeled with blue and yellow, shown above visualization of aligned reads for each group. Clearly demonstrating abundance of reads in Adult M and Juv M S, signifying peaks in the promoter region. **B)** qRT-PCR on selected genes show an upregulation in the Adult Male (blue), which has FoxP2 bound, compared to Adult F and Juv NS, which no FoxP2 binding was observed. FoxP2 expression (far right) implies FoxP2 binding is not due to increased abundance of FoxP2 in the Adult M.

Discussion

RNA-seq and ChIP-seq techniques provide a powerful means whereby one can identify changes in gene expression and transcription factor binding sites in an unbiased manner. Here, I was able to optimize the ChIP protocol to validate FoxP2 binding at specific sites and examine binding sites throughout the genome. One drawback, however, is that the large amount of data generates an abundance of noise. This is especially evident in the zebra finch model, where the amount of data far surpasses the genome's annotation. Yet, by closely examining the data, certain pathways or genes reveal themselves as avenues for further exploration. Our RNA-seq study provided a bioinformatic approach to identify genes correlated to learning to start deciphering possible pathways. By doing so, *MAPK11* was identified as having the greatest gene significance to vocal learning. The importance of FoxP2 to vocal learning led to the question of how FoxP2 influences *MAPK11* during this critical period.

Following optimization of the ChIP protocol, my ChIP-qPCR analysis in the zebra finch demonstrated FoxP2 binding to a region of *MAPK11*. Bioinformatic analysis suggested that this region was in the *MAPK11* promoter. Indeed, in a subset of animals that were previously generated, ChIP-qPCR results showed FoxP2 pulling down our *MAPK11* region of interest. However, when repeated on a new set of 12 birds via ChIP-seq, we failed to find a significant relationship. The sparsely annotated zebra finch genome makes it challenging to determine whether the *MAPK11* region in question lies in the promoter region, or within an intron. If so, this could explain the lack of evidence supporting FoxP2 regulation of *MAPK11* expression in both the new qPCR and Western analyses. If our hypothesis that FoxP2 is in fact binding to the promoter region, the absence of changes in expression upon FoxP2 overexpression may be due to the abundance of roles *MAPK11* plays within cell signaling cascades whereby a change in

one pathway may not be robust enough to be detected due to all the other regulatory signals. Indeed, there may be some type of compensatory regulation that resists the effects of our intervention.

The validation of the FoxP2-ChIP in zebra finch provides a novel look at which genes FoxP2 binds to in a laboratory model for vocal learning. Our analysis focused on differential FoxP2 binding sites associated with sex and developmental stage. The most interesting FoxP2 binding sites were specific to the adult male zebra finch. The RNA processing genes *RPL12*, *RPL22*, *RPL29*, and *RPL34* were found to be bound by FoxP2 only in the adult male. How these proteins regulate RNA translation throughout vocal development remains to be explored. RPL22 IP pulled down increased amounts of DARPP32, a marker for medium spiny neurons [55]. It is within these medium spiny neurons that is thought to be a key driver of FoxP2 expression in Area X [56]. This furthers the link by demonstrating medium spiny neurons express both FoxP2 and RPL22, with FoxP2 binding to and increasing the translation of RPL22.

Our analysis also highlighted *ATF4* as a FoxP2 target in adult males and juvenile singers. Meduim spiny neurons are GABAergic inhibitory neurons and ATF4 knockdown decreases $GABA_{\beta}R$ trafficking [54]. FoxP2 may regulate *ATF4* expression, affecting GABA receptor trafficking and neuronal firing rate. Area X plays a role in song modification and maintenance throughout the male zebra finch lifespan. FoxP2 binding to *ATF4* may play a role in a molecular pathways key to this vital song production behavior.

This project has highlighted a key technique to identify FoxP2 binding sites within the zebra finch model. Until the genome is fully annotated, these results are preliminary. The genes uncovered to be bound and regulated by FoxP2 provide further clues to the complex interplay of vocal learning and gene expression.

Appendix: FoxP2 Isoforms Delineate Spatiotemporal Transcriptional Networks for Vocal Learning in the Zebra Finch

Zachary D. Burkett, Nancy F. Day, Todd H. Kimball, Caitlin M. Aamodt, Jonathan B. Heston, Austin T. Hilliard, Xinshu Xiao, and Stephanie A. White

Statement of Contribution

Vocal learning in the zebra finch is accompanied by underlying changes in gene expression. In the song specific motor nucleus, Area X, of still learning juveniles, groups of interconnected genes are correlated to the act of learning and other groups to the act of singing. When compared to the gene expression network of adults, the connectiveness of singing correlated genes remains, while connectivity of the learning related gene modules breakdown. Those genes most correlated to singing can be mined for possible pathways partially responsible for the execution of song modification that must occur for song learning to be mastered. The work presented here is a study into these gene networks done by Zachary Burkett. My contribution to this was the beginning of my M.S. thesis, optimizing and performing a ChIP-PCR protocol in the zebra finch model and qRT-PCR. My contribution is presented in Figure A1C and Figure A6. I also wrote portions of the methods section that generated the data.

Abstract

Human speech is one of the few examples of vocal learning among mammals yet ~half of avian species exhibit this ability. Its neurogenetic basis is largely unknown beyond a shared requirement for FoxP2 in both humans and zebra finches. We manipulated FoxP2 isoforms in Area X, a song-specific region of the avian striatopallidum analogous to human anterior striatum, during a critical period for song development. We delineate, for the first time, unique contributions of each isoform to vocal learning. Weighted gene coexpression network analysis of RNA-seq data revealed gene modules correlated to singing, learning, or vocal variability. Coexpression related to singing was found in juvenile and adult Area X whereas coexpression correlated to learning was unique to juveniles. The confluence of learning and singing coexpression in juvenile Area X may underscore molecular processes that drive vocal learning in young zebra finches and, by analogy, humans.

Introduction

The ability to learn new vocalizations is a key subcomponent of language. Complex behaviors such as human speech and birdsong are rarely monogenic in origin, making the attribution of their direct molecular underpinnings a challenge (Marcus and Fisher, 2003). While language is unique to humans, learned vocal behavior is present in a number of animal taxa. Among laboratory animals, the zebra finch songbird (Taeniopygia guttata) is the primary genetic model for vocal learning, and song learning in this species shares numerous parallels with human speech development. For example, both species share corticostriatal loops for producing vocalizations and have direct projections from cortical neurons onto brainstem motor neurons that control the vocal organs, a connection that is lacking or reduced in non-vocal learners (Lemon, 2008; Ju¨rgens, 2002; Arriaga et al., 2012; Doupe and Kuhl, 1999; Petkov et al., 2012). The brains of avian vocal learners contain a distributed corticostriatal network of clustered cells devoted to vocal production learning, commonly referred to as the song control circuit, offering tractable targets for experimental manipulation. Despite their evolutionary distance, humans and zebra finches exhibit shared transcriptional profiles in key brain regions for vocal learning that are unique from surrounding brain areas and from the brains of non-vocal learning species (Pfenning et al., 2014).

The forkhead box P2 (FOXP2) transcription factor was the first gene shown to be important for vocal learning in both humans and songbirds. Forkhead box proteins are characterized by the presence of DNA-binding FOX domains (Clark et al., 1993) and FOXP subfamily members form homo- or heterodimers at zinc finger and leucine zipper domains in order to bind DNA. In humans, a heterozygous mutation in the FOX domain of FOXP2 causes a rare heritable speech and language disorder in a cohort known as the KE family (Vargha-

Khadem et al., 1998; Lai et al., 2001), potentially by altering the subcellular localization of the molecule (Vernes et al., 2006). While the mutation disrupts vocal learning (Marcus and Fisher, 2003) and also vocalization in vocal non-learners (Chabout et al., 2016; Castellucci et al., 2016), multiple FOXP2 isoforms are endogenous to both songbirds and humans, including one that lacks the DNA binding domain (Teramitsu and White, 2006; Bruce and Margolis, 2002). This truncated variant is referred to as FOXP2.10+ because, although it lacks the FOX domain, it retains the dimerization domains plus an additional 10 amino acids that are not found in the full-length form (FoxP2.FL).

Consistent with its lack of a FOX domain, in vitro assays of FOXP2.10+ indicate that it may regulate other FoxP2 isoforms (Vernes et al., 2006). Since it retains the dimerization domain, it has been hypothesized to act as a cytoplasmic sink, binding to other FOXP proteins and preventing their entry to the nucleus and interaction with DNA. Investigation of FoxP2 function in zebra finches has revealed remarkable parallels with humans. Similar FoxP2 expression patterns occur in developing human and zebra finch brains (Teramitsu et al., 2004). In zebra finches, knockdown of FoxP2 in the song dedicated striatopallidal nucleus, Area X, during vocal development impaired vocal mimicry of tutor songs (Haesler et al., 2007), much as the KE family mutation impairs speech. These observations indicate that functional FoxP2 is necessary for proper vocal learning, an inference supported by work in songbirds (Haesler et al., 2007; Heston and White, 2015).

The unique organization of song control circuit neurons enabled the discovery that FoxP2 is dynamically downregulated within Area X when zebra finches practice their songs, termed ‘undirected’ (UD) singing (Teramitsu and White, 2006; Miller et al., 2008; Hall, 1962; Immelmann, 1962; Dunn and Zann, 1996). This decrease in FoxP2 is accompanied by increased

vocal variability (Miller et al., 2010; Hilliard et al., 2012a), thought to be a form of vocal exploration. Blockade of FoxP2 downregulation impaired birds' ability to induce variability in their songs. A poor learning phenotype emerged following FoxP2 overexpression (Heston and White, 2015) that was remarkably similar to that observed following FoxP2 knockdown (Haesler et al., 2007). Taken together, these results indicate that the dynamic regulation of at least FoxP2.FL, and thereby the behavior-linked up- and down-regulation of its transcriptional targets, is necessary for the proper learning of vocalizations. No specific role in vocal behavior has yet been attributed to the FoxP2.10 + isoform.

These observations pinpoint FoxP2 as a molecular entry point to the pathways underlying vocal learning. In adult birds, we previously used Weighted Gene Coexpression Network Analysis (WGCNA) to identify thousands of genes regulated by singing specifically in Area X (Hilliard et al., 2012a; Langfelder and Horvath, 2008). Since adult zebra finches sing stable, or crystallized, songs, the transcription patterns underlying vocal learning were not identified. Here we conduct a new study with two goals: (1) Determine whether FoxP2.10+ may play a role in vocalization and, (2) Manipulate FoxP2 isoforms in juveniles to generate a broad range of behavioral and transcriptional states upon which to apply WGCNA and thereby reveal learning-related gene modules. Toward the first goal, overexpression of FoxP2.10+ revealed a unique role for this truncated isoform in the acute modulation of vocal variability. Toward the second goal, overexpression of either GFP or one of the two FoxP2 isoforms created three distinct groups of juvenile birds: one that was good at learning and acutely modulating variability (GFP), one that was poor at learning and acutely modulating variability (FoxP2.FL), and one that was good at learning but injected stability into song (FoxP2.10+). We applied WGCNA to the Area X transcriptome of birds across this behavioral continuum and discovered striatopallidal

coexpression patterns that were positively correlated to learning. These learning-related patterns were present in juvenile but not adult Area X. However, singing-driven coexpression patterns in Area X were largely preserved between juveniles and adults, suggesting that: (1) song production modules are independent of learning state and (2) the spatiotemporal cooccurrence of both song production and learning-related gene modules in juvenile Area X is fundamental to vocal learning.

Methods

Subjects

All animal use was in accordance with NIH guidelines for experiments involving vertebrate animals and approved by the University of California, Los Angeles Chancellor's Institutional Animal Care and Use Committee. Birds were selected from breeding pairs in our colony.

Experimental timeline

The experimental timeline is schematized in Figure 2A. Breeding cages that contained candidate experimental birds were placed in sound attenuation chambers along with their parents and siblings when juveniles reached ~20 d, as in Heston and White (Heston and White, 2015). Chambers were continuously recorded so as to capture tutor song. At 30d, juvenile males were bilaterally injected with AAV1 into Area X to overexpress either FoxP2.FL, FoxP2.10+, or GFP, then returned to their chambers. At 40d, juvenile males were isolated from all other birds and continuously audio-recorded. At ~60 d, an 'NS-UD' experiment was performed according to the methods of Miller et al., Chen et al., and Heston et al. (Heston and White, 2015; Miller et al., 2010; Chen et al., 2013) to assess the induction of vocal variability. On the 'NS-UD' day, for the first two hours after lights-on, birds were distracted by gentle 'shushing' if they attempted to sing. (Those that sang >10 motifs were excluded from that day's experiment). On the 'UD-UD'

day, birds were allowed to sing UD song for the first two hours after lights-on. The level of variability in songs sung subsequent to those two hours was quantified.

At 65d, birds were sacrificed following two hours of UD singing with one exception: In order to assure a broad range of song amounts immediately preceding sacrifice (and thereby capture a range of singing-induced gene expression), we distracted one bird in the GFP group from singing during the two hours preceding sacrifice.

A total of 19 birds received stereotaxic injections with AAV (7 GFP, 6 FoxP2.FL, 6 FoxP2.10+). Sample size was based on numbers used in Heston and White (Heston and White, 2015) where 5–8 animals per group were sufficient to reveal treatment effects. The authors of the WGCNA R package recommend a minimum of 15 samples for building a network (https://labs.genetics.ucla.edu/horvath/CoexpressionNetwork/Rpackages/WGCNA/faq.html), so we ensured at least five animals in each of the three groups.

Song recording

Countryman EMW or Shure SM93 omnidirectional lavalier microphones were used to continuously record birds from ~20 d until sacrifice (65d). Sounds were digitized using PreSonus FirePod or PreSonus Audioboxes at a 44.1 kHz sampling rate and 24-bit depth. Recordings were managed by SAP 2011 software (Tchernichovski et al., 2000).

Stereotaxic surgery and viruses

Behavior and RNA-seq experiments

As described in Heston and White (2015), 30d juvenile males were anesthetized using 2–4% isoflurane in pure oxygen and secured in a custom-built avian stereotaxic apparatus, then injected with virus bilaterally into Area X at the following coordinates: 45° head angle, 5.15 mm rostral of the bifurcation of the midsagittal sinus, 1.60 mm lateral of the midline, and to a depth of 3.3

mm. Virus was injected via a Drummond Nanoject II through a glass microelectrode (~40 mM inner diameter) backfilled with mineral oil. Three 27.6 nL injections were performed with a 15 s wait between injections and a 10 min wait before retraction of the electrode so as to minimize vacuum action pulling the virus away from the injection site. Incisions in the scalp were closed with Vetbond (3M, St. Paul, MN, USA). Birds received oxygen for ~2 min until alert, then returned to their home cages.

AAV1 used in Heston and White (Heston and White, 2015) and produced by Virovek (Hayward, CA) was used here. AAV1s contained zebra finch FoxP2.FL or FoxP2.10+ coding sequences (Teramitsu and White, 2006) (Genbank Accession Number DQ285023), or that for GFP, downstream of the CMV early enhancer/chicken b actin (CAG) promoter. Virus titers were all ~2.24E + 13 vg/ml, thus equivalent volumes were delivered to each bird irrespective of construct. Heston et al. (Heston and White, 2015) estimated that 24 ± 5.5% of neurons at the epicenter of the virus injection are transduced and that 96.7 ± 1.7% of cells that are transduced are neurons. These transduction rates are sufficient to observe a behavioral effect of the virus and were thus used in the present study.

Histological assessment of FoxP2.10+ overexpression

FoxP2.10+ is a naturally occurring truncated isoform of FoxP2.FL, with a unique 10 amino acid sequence at its C-terminus. There is currently no antibody specific to this truncated isoform, presenting a challenge to its immunological detection. The limited cloning capacity of AAV precluded our ability to express a reporter gene in the viruses that we used for behavioral and RNA-seq experiments. Moreover, we opted not to include an epitope tag on AAV-expressed FoxP2 isoforms in order to avoid any conformational changes that could confound our behavioral or RNA-seq analyses. For histological analysis only, however, we took advantage of

the larger cloning capacity of HSV to express FoxP2.10+ tagged with an Xpress epitope at its N-terminus downstream of the IE 4/5 promoter and a GFP transduction reporter downstream of the CMV promoter (McGovern Institute for Brain Research at the Massachusetts Institute of Technology, Cambridge, MA). Surgical procedures were identical to those performed with AAV except that the virus was diluted to 60% in PBS immediately preceding injection, per the manufacturer's recommendation. HSV reaches peak expression more rapidly than does AAV, thus HSV-injected birds were sacrificed 3–5 days post-injection (Neve et al., 2005).

In situ hybridization

In situ hybridizations were performed as in Jacobs et al. (1999) using two [33P]UTP-labeled riboprobes antisense to distinct regions of zebra finch FoxP2 (Teramitsu et al., 2004). 20 mM thick sections were thaw-mounted onto Superfrost Plus microscope slides (ThermoFisher Scientific, Waltham, MA, USA), then postfixed with 4% paraformaldehyde in PBS, pH 7.4.

PCR primers

To quantify levels of FoxP2.FL, we selected a primer pair previously used to quantify FoxP2 knockdown (Haesler et al., 2007; Olias et al., 2014). The forward sequence was 5'-CCTGGCTG TGAAAGCGTTTG-3' and the reverse was 5'ATTTGCACCCGACACTGAGC-3'. We designed a primer pair for FoxP2.10+ using the NCBI Primer-BLAST tool (Ye et al., 2012). The input sequence was FoxP2.10+ mRNA CDS (GenBank accession DQ285023.1). The forward primer sequence was 5'-CGCGAACGTCTTCAAGCAAT-3' and the reverse sequence was 5'-AAAGCAATATGCACTTACAGGTT-3'. Primer specificity was determined by obtaining a single peak in melting curve analysis and obtaining a single amplicon of predicted size following qPCR. GAPDH forward and reverse primers were 5'-AACCAGCCAAGTACGATGACAT-3' and 5'-CCATCAGCAGCAGCCTTCA-3', respectively.

qRT-PCR experiments

200 ng of RNA from Area X micropunches was reverse transcribed into cDNA using the Bio-Rad iScript cDNA Synthesis Kit (Hercules, CA, USA). 25 mL qPCR reactions were assembled in MicroAmp Optical 96-Well Reaction Plates (ThermoFisher Scientific). Reaction components were 0.5 mL cDNA, 200 nM primers, 12.5 mL PowerUp SYBR Green Master Mix (ThermoFisher Scientific), and 10.75 uL nuclease-free water. Cycling conditions were 50°C for 2 min, 95°C for 2 min, then 40 cycles of 95°C for 15 s and 60°C for 1 min. A dissociation step of 95°C for 15 s, 60°C for 1 min, 95°C for 15 s, and 60°C for 15 s was then performed. All reactions were run in triplicate and all samples for an individual animal were run together on the sample plate. FoxP2 expression was quantified relative to GAPDH and normalized to the GFP-injected animals using the 2-D DCT method (Livak and Schmittgen, 2001).

Immunostaining

For histological analyses, animals were sacrificed 3–5 days following HSV injection then perfused with warm saline followed by ice cold 4% paraformaldehyde in 0.1 M phosphate buffer. Tissue was cryosectioned at 20 mM, thaw-mounted onto glass microscope slides, and stored at -80°C until use. Thawed sections were incubated overnight with goat-anti-FoxP2 (1:500; Abcam, Cambridge, UK; [Thompson et al., 2013]) and mouse-anti-Xpress (1:500; ThermoFisher Scientific, Waltham, MA). AlexaFluor 546 donkey-anti-goat (1:500) and AlexaFluor 405 donkey-anti-mouse (1:250) secondary antibodies were used to generate anti-FoxP2 and anti-Xpress signals, respectively. Sections were visualized using a Zeiss (Oberkochen, Germany) LSM 800 confocal microscope and processed using NIH ImageJ (Schneider et al., 2012).

Song analysis and statistics

Motif similarity

The Similarity Batch in SAP was used to quantify the acoustic similarity between pupil and tutor songs (Tchernichovski et al., 2000). Asymmetric comparisons were performed between 10 tutor motifs (obtained from the final day before the pupil was acoustically isolated) and 20 pupil motifs (obtained every ~3 days following viral injection). We used the average percentage similarity from these comparisons as a representative of how well the pupil learned its tutor's song on a given day of analysis. Statistical significance of motif similarity data was calculated by performing one-way ANOVAs on the average percentage similarity score of each animal across virus groups within each time bin, as depicted in Figure 2D. If the ANOVA yielded a significant result, Tukey's Honest Significant Difference (HSD) was used as a post-hoc test.

Overall vocal variability

To broadly assess the amount of variability in the animal's song preceding sacrifice, asymmetric comparisons between 20 pupil motifs and themselves were conducted. We calculated the motif identity for all motif-motif comparisons as the product of their percentage similarity and accuracy divided by 100. Higher identity scores indicate lower variability within the batch.

Acute vocal variability modulation

For finer-grained analyses of acoustic variability as presented in Figures 2C and Figure 2—figure supplement 1, we utilized SAP and Vocal Inventory Clustering Engine (VoICE; [Burkett et al., 2015]; https://github.com/zburkett/VoICE). Syllables from the first 20 min following two hours of non-singing or undirected singing on the NS-UD experiment days were hand segmented, had their acoustic features quantified in the SAP Feature Batch, then clustered by VoICE. Data for analyses of acoustic features were taken from the VoICE output. Effect sizes were calculated using the formula (NS-UD)/(NS +UD), where values were the CV of a given

acoustic feature following two hours of NS or UD. Thus, negative values indicate increased song variability after UD singing (see below for more information regarding this transformation). Statistical significance for each song feature was assessed by one-way ANOVA on the CV effect size for all syllables from all animals within each group. Tukey's HSD was used as a post-hoc test in the instance of a significant ANOVA result. For the raw acoustic data, as presented in Figure 2—figure supplement 1, the syllables were considered paired within virus construct and across singing context. Paired T-tests were used to assess whether two hours of non-singing vs. two hours of undirected singing significantly altered the CV for each acoustic feature.

Song analysis: (NS-UD)/(NS + UD) effect size vs. raw acoustic feature CV

The calculation of effect size was performed because it allows for comparison across virus groups instead of a series of paired comparisons within group (Miller et al., 2015). The transformation normalizes acoustic features so that any observed changes are viewed in the context of the initial values. We present a hypothetical example in the table below where a change of 50 Hz for two syllables is given a greater weight for a syllable that has an overall lower frequency when using the transformation we applied for our song data:

Syllable A				Syllable B			
NS	UD	Raw Delta	(NS-UD)/(NS+UD)	NS	UD	Raw Delta	(NS-UD)/(NS+UD)
100 Hz	150 Hz	50 Hz	-0.2	500 Hz	550 Hz	50 Hz	-0.048

Tissue collection and processing, RNA extraction, cDNA library preparation, and sequencing

Two hours following lights-on at ~65 d, birds were sacrificed by decapitation. Brains were rapidly extracted and frozen on liquid nitrogen, then stored at -80°C until all brains were collected. As in Hilliard et al. (2012a), tissue micropunches of Area X and VSP were performed. Brains were coronally sectioned on a cryostat at 30 mM until Area X became visible. Area X and outlying VSP were punched using a 20-gauge Luer adapter and stored in RNAlater (Qiagen,

Germantown, MD) at -80°C until RNA extraction was performed. 30 mM sections were then collected, thaw mounted, and thionin stained for post-hoc validation of punch accuracy.

Total RNA extraction was performed as in Hilliard et al. (2012a). Samples were processed semi-randomly and in parallel with another sequencing project. Tissue punches from both studies were processed in batches of 8. We used Qiagen RNeasy Micro Kits (Cat. No 74004) following the manufacturer's protocol and QIAzol as the lysis reagent. An additional wash beyond the manufacturer's protocol was performed in RW1 and RPE buffers. Final elution volume was 20 mL. Extracted total RNA were stored at -80°C until all RNA extractions were completed. All extractions were completed over the course of two weeks.

Total RNA was provided to the UCLA Neuroscience Genomics Core (UNGC; https://www.semel.ucla.edu/ungc) where RNA quality was assessed on an Agilent TapeStation (Agilent Technologies, Santa Clara, California). RNA of sufficient quality (RIN >8) was then used to generate cDNA libraries using the Illumina TruSeq Stranded Poly-A Prep Kit (Illumina, San Diego, CA, USA Cat No 20020594). Libraries for each sample were divided across two lanes and sequenced in a total of 8 lanes using an Illumina HiSeq 2500 in high output mode, generating between 15 and 35 million 50 bp paired-end reads per library.

RNA-seq preprocessing and WGCNA

Raw FASTQ files furnished by UNGC were first quality controlled using FASTQC (http://www.bioinformatics.babraham.ac.uk/projects/fastqc/). FASTQC returned results indicating high quality across all bases in each read in each sample and no adapter contamination was detected, therefore we did not perform any filtration of the reads before alignment. Reads were aligned to the NCBI zebra finch genome assembly 3.2.4 (http://www.ncbi.nlm.nih.gov/assembly/524908/) and RefSeq annotations using STAR (Dobin et

al., 2013). Mismatch tolerance was two base pairs. Only uniquely mapped reads were considered in downstream analyses. The featureCounts() function in the Rsubread R package was used to count all reads mapping within exon features, then all exon counts were summed to the gene level so that each gene had a single value of reads mapped to it (Liao et al., 2014; Liao et al., 2013). Gene expression was then quantified by calculation of transcripts per million (TPM). TPM values were log2 transformed and genes with zero variance across samples were removed. We checked for batch effect on average expression resultant of RNA extraction group, RNA extraction experimenter, and across sequencing lanes. No batch effects were observed. We used an iterative process of removing gene expression data from single samples whose expression was >2.5 SD of that gene's expression across all samples, repeating until no samples remained with expression >2.5 SD away from the gene's average expression across all samples. Finally, we calculated the intrasample correlation (ISC) and used a hard cutoff of 2 SD away from the group ISC for removal of samples from the study. No sample in any group (Area X or VSP) was >2 SD from the group ISC. Data were quantile normalized as the last step. Final data input to WGCNA was 13665 and 13781 genes for Area X and VSP networks, respectively, across 19 total samples. We calculated the soft thresholding power for construction of the WGCNA adjacency matrix using the pickSoftThreshold function in the WGCNA R package at 18 for Area X and 14 for VSP. We then constructed a signed network using the blockwiseModules function in the WGCNA R package. For the Area X network, we used a minimum module size of 100 genes and deepSplit was set equal to four for Area X and two for VSP. Genes were required to have at least a connectivity of 0.3 with their module eigengene in order to remain a member of their module and the module 'core' (=minimum module size/3) needed to have a minimum eigengene connectivity of 0.5 for the module to not be disbanded. All other parameters were set to default.

Networks were iteratively constructed with genes in the grey module removed from the expression data after each round of network building and module definition. The networks were considered final after no genes were placed into the grey module.

During network construction, FoxP2 was removed, presumably due to the lack of coexpression with other genes in the network resulting from virus-driven overexpression. Therefore, we added FoxP2's expression data back into the final overall network and it became the only gene in the grey module. Once coexpression modules were defined, we correlated vocal behavior to the module eigengenes. Since the grey module included only a single gene with no significant behavioral correlations, it was excluded from module-trait analyses.

WGCNA and network terminology

WGCNA is a well-established technique for gleaning biologically relevant clusters of coexpressed and functionally related genes from microarray and sequencing data. WGCNA methods and terminology are summarized and defined in numerous manuscripts (Hilliard et al., 2012a; Zhang and Horvath, 2005; Dong and Horvath, 2007; Zhao et al., 2010; Yip and Horvath, 2007; Horvath, 2011). For the sake of convenience, we provide working definitions of network terms that we use throughout the manuscript. Definitions of greater detail are available in the manuscripts cited above.

- Adjacency (a): The first step of network construction is to generate an adjacency matrix where $A_{ij} = S_{ij}^{\beta}$, where i and j are genes, S is the expression correlation across samples, and β is an empirically derived power to which the correlation is raised such that the resulting network approximates a scale free topology.
- Connectivity (k): Connectivity is a measure of connectedness of a given gene, either in the context of its module (kIN) or the entire network (kTotal). Connectivity is defined as

follows: $k_i = \sum_{j=1}^{N} a_{ij}$ where i and j are genes, N is all of the genes in the module or network, and a is the adjacency between genes i and j.

- Topological overlap: Adjacency is transformed to topological overlap as a method of calculating the interconnectedness (or similarity) between two nodes. Topological overlap is defined as follows: $\omega_{ij} = (l_{ij} + a_{ij})/(\min\{k_i,k_j\} + a_{ij})$ and $l_{ij} = \sum_{u \neq i,j} a_{iu} a_{uj}$ where u represents all genes besides i and j. A and k are defined above.
- Gene significance: The Pearson correlation between a gene's expression profile and, in our work, a given behavioral metric.
- Module eigengene: The first principal component of a module's gene expression profile, a method of summarizing an entire module in one vector.
- Module membership: The correlation between an individual gene expression profile and a module eigengene. Genes with high module membership tend to have high intramodular connectivity and are referred to as intramodular hubs. Of note, genes can have high module membership in more than one module.
- Zsummary: Along with median rank, a term for quantifying preservation of gene coexpression patterns between two independent datasets (Langfelder et al., 2011), such as between juvenile and adult Area X or juvenile Area X and juvenile VSP. Zsummary is a composite preservation score defined as the average of Zdensity and Zconnectivity, which assess the preservation of connection strength among network nodes (e.g. Are strongly connected nodes in one network also strongly connected in the other?) and the connectivity patterns between nodes (e.g. Do the patterns of connection between specific nodes exist in both networks?), respectively, following permutation tests under the null hypothesis. Higher Zsummary scores indicate better preservation.

Correlation of behavior to gene expression

Calculation of gene significance to a trait requires the definition of a single value to which the amount of gene expression in each sample is correlated. Gene significances were calculated for the following traits: Motifs, defined as the number of motifs each animal sang in the two hours following lights-on on the day of sacrifice; Tutor similarity, defined as the percentage similarity between the pupil and its tutor on the day of sacrifice; Variability induction, defined by inserting Wiener entropy CV scores into the equation (NS-UD)/(NS + UD) from the first twenty syllable renditions sung during the NS-UD experiment performed at ~60 d; Motif identity, defined as the product of the similarity and accuracy scores divided by 100 of the last 20 motifs sung by each bird before sacrifice. Song variability was assessed on the motif level for the purpose of gene significance calculations so as to obtain a single value for each animal.

Following network construction, modules were summarized by calculating a module eigengene, defined as the first principal component of the module's expression data using the moduleEigengenes() function in the WGCNA R package. The relationship between a module and a behavior was assessed by determining the Pearson correlation between the module eigengene and continuous behavioral traits as defined in 'Song Analysis and Statistics', above. Significance was then determined by calculating the Fisher transformation of each correlation using the corPvalueFisher() function in the WGCNA R package. We performed p-value corrections for module-trait correlations using the p.adjust() function with the number of comparisons equal to the number of traits (4) by the number of modules (21; the FoxP2-only grey module was not included for purposes of p-value correction). The p-values presented in this manuscript are uncorrected for multiple hypothesis testing but those that pass FDR-correction at $p<0.05$ are indicated. We chose to present uncorrected p-values due to the small sample size used

to create the overall network (n = 19 birds). The authors of WGCNA suggest a minimum of 15 samples with >20 preferred (https://labs.genetics.ucla.edu/horvath/CoexpressionNetwork/Rpackages/WGCNA/faq.html). P-value corrections drive nearly all results to insignificance, including well preserved module-trait relationships that are present in adults and survive such corrections due to the larger sample size in that study. We use the significant but uncorrected p-values in this study as a guide toward interesting module-trait relationships, then use the properties of the network to inform the downstream analysis.

Our choice of behavioral traits for correlation to the gene network was hypothesis-driven. In addition to the obvious quantification of vocal learning, the comparison for variability induction was planned, as indicated by the fact that we conducted the NS-UD and UD-UD behavioral paradigms (prior to the bird's sacrifice) that led to it. We originally used these paradigms as a method for naturally regulating FoxP2 levels, before we had identified a virus that was effective in doing so. In that study (Miller et al., 2010), our prediction was that behavioral conditions that lead to low endogenous FoxP2 in Area X (namely 2 hr of UD singing), would be associated with higher levels of variability. This was indeed the case. We replicated this finding in zebra finches (Heston and White, 2015) but did not observe the same phenomenon in Bengalese finches (Chen et al., 2013) as noted in our Discussion. The feature highlighted by those studies was Weiner entropy.

Gene ontology, module significance, and term significance

At the time of this study, annotation of the zebra finch genome is relatively sparse, thus zebra finch gene symbols were converted to their Human Genome Organisation (HUGO) Gene Nomenclature Committee (HGNC) paralogs, then submitted to GeneAnalytics, a comprehensive

tool for the contextualization of gene set data that integrates across multiple databases (Ben-Ari Fuchs et al., 2016). Genes with no known human homolog were excluded. Symbols were submitted to the GeneCards GeneAnalytics suite at http://geneanalytics.genecards.org (Ben-Ari Fuchs et al., 2016). GeneCards enrichment scores were converted into p-values, which were used as the input to module significance calculations. Module significance of a term was defined as the product of the average module membership for each gene annotated with a term, and one minus the p-value for that term such that the genes with the highest module membership and lowest p-value prioritize the terms (Hilliard et al., 2012a). Term significance was defined by weighting the module significance score by the gene significance for a given behavioral metric.

Transcription factor binding site analysis

The FoxP2 consensus binding sequence from the JASPAR database (Nelson et al., 2013; Mathelier et al., 2016) was converted into a position-weight matrix (PWM) and used to scan the promoter (defined as the first 1000 base pairs upstream of the transcription start site in the RefSeq models) for each gene in the zebra finch genome. Putative FoxP2 binding sites were identified using the matchPWM function in the Biostrings R package (https://bioconductor.org/packages/release/bioc/html/Biostrings.html) with a minimum hit score of 80%.

Chromatin immunoprecipitation-PCR

Chromatin immunoprecipitation (ChIP) was performed using ChIP-IT High Sensitivity (Active Motif, Carlsbad, CA, USA, Cat. No. 53040) following the manufacturer's protocol. Whole brain was isolated from an adult male zebra finch, minced, and crosslinked in a formaldehyde solution. The tissue was homogenized with a hand-held tissue homogenizer for 45 s at 35,000 rpm. Following homogenization, the sample was sonicated at 25% amplitude 30 s on, 30 s off, for 10

min. A portion of the sonicate was de-crosslinked and quantified. The sample was split evenly into three tubes. A cocktail of anti-FoxP2 primary antibodies were applied to one sample (Millipore, Billerica, MA, USA Cat. No. ABE73, ThermoFisher Scientific Cat. No. 5C11A2, and Abcam ab16046), IgG in another (Millipore 12–370), and the third was input DNA. After an overnight incubation, the samples were washed, decrosslinked and subjected to PCR. The 'promoter' sequence for *MAPK11* was binned into 100 bp regions for primer construction. *MAPK11* primers were as follows: forward 5'- CCCTTTCCCCAAATGGCAGA-3' and reverse 5'-TATGAGCCTTGCCTTGGAGC-3'. PCR protocol was performed using DreamTaq PCR Master Mix per manufacturer's protocol. A PCR protocol was used as follows: (1) 95°C 1 min, (2) 95°C 30 s, (3) 67°C 30 s, (4) 72°C 1 min, repeat (2-4) for 40 cycles, (5) 72°C 10 min. PCR products were run on a 1.5% agarose gel in the presence of SYBR Safe to allow visualization of DNA. PCR products were purified (QIAQuick Gel Extraction Kit) and sent for sequencing by Laragen, Inc. Reverse primers sent for sequencing are as follows: 5'-TATGAGCCTTGCCTTGGAGC-3' and 5'-CCTATGAGCCTTGCCTTGGA-3'.

Protein interaction networks and scaling of interaction confidence scores

STRING is a comprehensive database of known and predicted protein-protein interactions derived from experimental data, coexpression data, automated text mining, and also pulls information from other interaction databases. STRING accepts gene symbols as input, then mines for interactions between those genes and assigns a confidence score between 0 and 1 based on the evidence in the database for the genes' interaction. We submitted gene symbols for the human homologs of module members to STRING then operated on the highest confidence interactions ($\geq$0.9) in downstream analyses.

Interaction scores were scaled by different metrics to emphasize or deemphasize network position and/or relationship to behavior (Supplementary file 5). Those metrics are:

1. The product of each gene's connectivity in juvenile Area X network: emphasizes interactions between the most connected genes in the juvenile network.
2. The product of each gene's differential connectivity between juvenile and adult Area X networks: emphasizes interactions between genes that are of high network importance in juveniles but not adults.
3. The product of each gene's gene significance for learning or singing: emphasizes interactions between genes that are strongly correlated to behavior independent of their connectivity.
4. The product of each gene's connectivity and gene significance: emphasizes interactions between genes that are strongly correlated to behavior and of highly connected in the juvenile network.

Network visualization and interactive figures

Network plots presented in this manuscript were constructed using the freely available plotting software, Gephi (https://gephi.org), using edge lists prepared in R and exported in the. GEXF format.

We have created interactive versions of many of the network plots in this manuscript (Figure 3F) all additional Area X modules (similar to Figure 3F but not presented in the manuscript), and the protein interaction network presented in Figure 7. They are hosted at our laboratory website (https://www.ibp.ucla.edu/research/white/genenetwork.html) along with high resolution static PDF versions. Interactive figures were exported from Gephi using the Sigma.js Exporter plugin (https://github.com/oxfordinternetinstitute/gephi-plugins).

In weighted coexpression networks, each node (i.e. gene) is connected to every other node in the network, even if the weight of the edge (i.e. connection) is zero. Therefore, plots depicting nodes and their edges with other genes become exceedingly complicated and unintuitive if all nodes and edges are included. In an effort to sparsify the networks and present the most salient data, we removed edges and genes from the coexpression networks using the following workflow: first, remove $\leq$98% of edges, then remove all disconnected nodes, then remove all nodes that are not part of the network's main component (e.g. the largest group of connected nodes). The remaining nodes and edges were plotted.

In this manuscript, we present three types of network plots that look similar but convey different data. The three types are as follows:

1. The overall gene coexpression network, as in Figure 3—figure supplement 5 and https://sites.google.com/a/g.ucla.edu/genenet/coexpressionnetwork. In these plots, the nodes represent genes and their colors represent the module assignment. Edges represent the adjacency between nodes and the edge color is a combination of the origin and target node colors. Due to the overwhelming number of edges in this network, the edge weights are scaled to minimize the range. Node size in this network is equivalent to the node's degree (e.g. the number of connections originating or terminating at that node) and the maximum node size is suppressed so as to provide maximal visual clarity.

2. Individual coexpression modules, as in Figure 3F and https://sites.google.com/a/g.ucla.edu/genenet/modules. These plots are similar to the preceding except that, potentially, more nodes are present in the module since the filtration procedures detailed above are applied in a different context (e.g. only the expression data in the module are

considered here vs. the expression data for the entire network). The same scaling parameters as above are applied to the edges for visual clarity.

3. Protein interaction network, as in Figure 7 and https://sites.google.com/a/g.ucla.edu/genenet/protein. Nodes represent proteins and their colors represent the coexpression module assignments. Node size is equivalent to its degree. Here, the edge width conveys meaning and is helpful in interpreting the relationship between nodes. An edge is drawn between two nodes when the STRING database indicates a high confidence interaction (score $\geq$0.9) between them. Edge widths are the confidence score scaled by the product of the origin and target node's intramodular connectivities (kIN). Thus, thick edges indicate a high confidence protein level interaction between two genes that are well connected members of learning and singing related modules. Unlike the previous plots, a node's size does not necessarily convey a higher degree of coexpression network importance. Instead, it indicates many interactions involving this protein described in the database. The thickness of the edges conveys influence of the gene's biological importance, as interpreted through their kIN. Whether a node's degree or the weight of its connections is the ultimate determinant of its relationship to vocal learning remains to be determined but the reader should keep the preceding information in mind when interpreting this network.

Accession information

Raw and processed RNA-seq and behavioral data for each bird are available at the Gene Expression Omnibus (GEO; https://www.ncbi.nlm.nih.gov/geo/) at accession number GSE96843.

Results

Virus-mediated overexpression of FoxP2 isoforms affects song learning and/or vocal variability

Adeno-associated viral (AAV) constructs were used to drive overexpression of FoxP2.FL or FoxP2.10+ in Area X of developing males (Figure 1—figure supplement 1). To verify isoform-specific overexpression, we used two riboprobes in in situ hybridization experiments: one antisense to a region common to both transcripts (mid probe) and one antisense to a region near the 3' end of FoxP2.FL (3' probe; [Teramitsu and White, 2006]; Figure 1A). Robust signals beyond endogenous/background levels were observed in the striatopallidum of both hemispheres using the mid probe but only in the hemisphere injected with the FoxP2.FL construct using the 3' probe (Figure 1B). These results indicate that each viral construct overexpressed its encoded FoxP2 isoform and was thus suitable for bilateral injection into Area X of juvenile males at 35d. An additional cohort received AAV encoding GFP as a control. We quantified levels of FoxP2 expression at 65d by performing qRT-PCR with a set of primers that amplifies a region common to both transcripts (Haesler et al., 2007; Olias et al., 2014) and another set specific to the FoxP2.10+ (see Materials and methods). The first primer set indicated that FoxP2 levels were higher in birds injected with either construct relative to control levels. When quantified by the second primer set, we found elevated PCR product only in the animals injected with the FoxP2.10+ construct (Figure 1C). No overexpression was detected in the ventral striatopallidum (VSP; the zebra finch striatum is interspersed with pallidal-like cells and is separate from the pallidum [Reiner et al., 2004]) (Figure 1—figure supplement 2). Taken together, these results indicate that both constructs were effective in elevating levels of their encoded FoxP2 isoform within Area X throughout the 30d experimental period.

Overexpression of a tagged form of FoxP2.10+ in a human neuronal cell line (SH-SY5Y) suggested that FoxP2.10+ acts as a posttranslational regulator of FoxP2.FL through heterodimerization and the formation of cytoplasmic aggresomes (Vernes et al., 2006). We thus examined the protein-level distribution of FoxP2.10+ and FoxP2.FL in the finch striatopallidum following overexpression of an N-terminus Xpress tagged FoxP2.10+ linked to a GFP reporter (see Stereotaxic Surgery and Viruses in Materials and methods). Transduced cells shared the distinctive FoxP2.10+ staining pattern of aggresomes seen previously. In FoxP2+ cells that co-expressed the Xpress tag and GFP reporter, endogenous FoxP2.FL signal was interspersed among Xpress-positive puncta (Vernes et al., 2006) (Figure 1D).

We previously found that, in unmanipulated birds, two hours of UD singing in the morning is sufficient to decrease Area X FoxP2 mRNA (as measured by both the mid and 3' probes) and protein (Teramitsu and White, 2006; Miller et al., 2008). This decrease in FoxP2 was accompanied by an increase in the variability of UD songs, in the form of decreased self-similarity (see Materials and methods), that were sung subsequent to the two hour time-point, a paradigm which we term UD-UD (Miller et al., 2010; Hilliard et al., 2012a). In contrast, when birds were distracted from singing for two hours in the morning (non-singing; NS), their subsequent UD songs (termed NS-UD) were less variable. Moreover, overexpression of FoxP2.FL in Area X abolished the increase in vocal variability normally induced by the UD-UD paradigm (Heston and White, 2015). These observations indicate that downregulation of full length FoxP2 is important for acute vocal variability but we did not directly manipulate FoxP2.10+. Here, we performed similar behavioral experiments to test for the induction of vocal variability and included the FoxP2.10+ injected animals (Figure 2A and B). To assess whether UD singing drove an increase in vocal variability, we used the UD-UD paradigm (see Materials

and methods) and quantified the effect of two hours of UD singing on the coefficient of variation (CV) of acoustic features in the subsequent UD songs of ~60d birds overexpressing GFP, FoxP2.FL, or FoxP2.10+. Results were compared to songs sung by the same birds undergoing the NS-UD paradigm. As predicted, GFP-expressing animals exhibited a negative effect size for most acoustic features, and FoxP2.FL overexpression diminished these practice-induced changes in vocal variability, replicating our previous findings (Heston and White, 2015) (Figure 2C).

Unexpectedly, in animals overexpressing FoxP2.10+, song variability after two hours of UD singing (UD-UD) was significantly less than that after two hours of non-singing (NS-UD) for syllable duration, amplitude modulation, and Wiener entropy (Figure 2C). Rather than increasing song variability (as in the GFP group) or creating a state of equivalent variability (as in the FoxP2.FL group), UD-UD singing led to markedly invariable songs in the FoxP2.10+ birds, suggesting a role for FoxP2.10+ in promoting song stability. We also examined variability in the raw acoustic features of NS-UD and UD-UD song and found that expression of either FoxP2 isoform did not dramatically alter variability, indicating that the viral-driven overexpression specifically affected the modulation of variability (See 'Acute Modulation of Vocal Variability' in Materials and methods) and not its overall level (Figure 2-figure supplement 1 and Materials and methods). Despite its suppressive effect on practice-induced song variability, overexpression of FoxP2.10+ did not impair overall vocal learning (Figure 2D and E). As shown by Heston and White (Heston and White, 2015), FoxP2.FL birds were capable of changing their songs over the course of the experiment (data not shown) but were less able to match their tutors' songs (Figure 2D and E). These results suggest that the ability to modulate between relatively low and high variability states is important for proper vocal learning.

In sum, our viral manipulations generated groups of animals in distinct states of vocal variability and learning. GFP-injected birds learned well and displayed singing-induced variability in the acoustic features of song. FoxP2.FL birds learned poorly and had no difference in their songs' acoustic variability following practice. FoxP2.10+ birds learned well but seemed to exist in a state where practice drives invariability in vocal acoustics. As such, a broad degree of both learning and variability induction existed across groups (Figure 2F). Next, we used these behavioral metrics as correlates to gene coexpression patterns to interrogate the transcriptional profiles underlying these traits.

Gene modules in juvenile Area X that correlate to vocal behavior are enriched for communication and intellectual disability risk genes

We used RNA-seq to quantify gene transcription in Area X of 65d juveniles overexpressing GFP, FoxP2.FL or FoxP2.10+, then used WGCNA to identify gene coexpression modules and link them to song learning. We built an overall network composed from all samples together (Figure 3A and B), as well as construct-specific networks (Figure 3—figure supplements 1–4). In the overall network (see Materials and methods), 7461 genes formed 21 modules (Figure 3A and B, Supplementary file 1). We found significant correlations between module eigengenes and the following behaviors: tutor percentage similarity (i.e. vocal learning: darkred, green, and greenyellow modules), number of motifs sung (i.e. amount of singing: black, orange, darkgreen, royalblue, and blue modules), singing-induced acoustic variability (i.e. variability induction: black, brown, darkgreen, darkgrey, magenta, orange, pink, purple and turquoise modules), and motif identity (i.e. overall vocal variability: dark-grey module) ($0.00008 < p < 0.05$; Figure 3B). Hereafter, these modules are termed 'learning-related', 'song-production', 'variability-induction' and 'vocal variability' modules, respectively. We examined all modules whose p-value was

≤0.05 and calculated the relationship between module membership and gene significance. (For definitions of WGCNA and network terms, see Materials and methods: WGCNA and network terminology. For information about significance levels reported here, see Materials and methods: Correlation of behavior to gene expression). For most modules, strong correlations were observed for each trait, indicating that the genes most representative of the module's overall expression profile were those most strongly related to the behavior (Figure 3C).

Connectivity is the core gene coexpression network concept and genes with high connectivity have the strongest coexpression relationships across the entire network, indicating greater importance to overall network structure and biological significance. The purple, green, and pink modules contained the most densely interconnected genes (Figure 3—figure supplement 5), and were correlated to percentage similarity to tutor (green learning-related module) or singing-induced variability (purple and pink variability-induction modules) (Figure 3B and D). These findings indicate that information about the relationships between gene coexpression and behavior was reflected in the structure of the network: A gene's relationship to a module or a module's relationship to the network was predictive of strong behavioral relevance. Therefore, we examined the most well-connected/hub genes within the context of their module (genes with the greatest intramodular connectivity) or the entire network (genes with the greatest whole-network connectivity). We discovered that many of these hub genes are known risk genes for human disease. For example, of the 7462 genes in the overall network, Fragile X Mental Retardation 1 (FMR1) had the third highest connectivity and was the most well connected member of the green module (Supplementary file 1). Deficiency in FMR1 gives rise to Fragile X Syndrome, a genetic disease with a multitude of symptoms including intellectual deficiency and speech and language impairment.

To attribute biological meaning to the modules, we calculated a module significance score for the resulting disease, gene ontology, and pathway annotations returned from GeneAnalytics (Ben-Ari Fuchs et al., 2016) (See Materials and methods). The top five terms for the black song production module (negatively correlated to the amount of singing), the brown variability induction module (positively correlated to variability induction), and green learning-related module (positively correlated to learning) are shown in Figure 3E with comprehensive results presented in Supplementary file 2. Since most modules contain hundreds of genes, prioritizing the ontology terms by the connectivity of their annotated genes allows genes with the greatest network importance (Figure 3F) to emphasize the terms with the greatest biological importance (Figure 3E).

Juvenile Area X modules for learning, but not singing, are preserved in juvenile VSP

To validate the specificity of the Area X modules to vocal behavior, we compared the overall Area X network to a network constructed from the adjacent non-song VSP (Hilliard et al., 2012a; Feenders et al., 2008) from the same animals. Area X and VSP networks were constructed using the genes that were common to the two, enabling analysis using module preservation functions. We hypothesized that the genes in the Area X song production modules would have no correlation to behavior in VSP since, despite its close proximity and similar cell type composition, the VSP is not similarly linked into song control circuitry (Person et al., 2008). Moreover, a body of evidence suggests that the song control circuit evolved as a specialization of existing motor circuitry (Pfenning et al., 2014; Feenders et al., 2008; Barrett, 2012; Oakley and Rivera, 2008). As predicted, no module in the VSP network displayed any correlation to any of the singing or learning behaviors as gene significances using Area X and VSP expression data are markedly different (Figure 4A, X vs. V). We calculated module preservation statistics

between the two brain regions and observed that the song production modules were among the most poorly preserved (Langfelder et al., 2011) across the two networks (Figure 4B, Supplementary file 3). This result indicates differential connectivity of song production module genes between Area X (Figure 4C, top) and VSP (Figure 4C, bottom), further underscoring that Area X is specialized for song. This lack of preservation was not the product of differential gene expression between the two regions (Figure 4D, top) but instead reflected altered connectivity among similar genes (Figure 4D, bottom). In striking contrast to the song production modules, the green learning-related module was strongly preserved in VSP (Figure 4B, Figure 3B), indicating a generalized learning-related coexpression state exists in the juvenile striatopallidum that is specialized for singing in Area X.

Juvenile Area X modules for singing, but not learning, are preserved in adult Area X

To provide further context for the modules observed in our overall network and how they relate to learned vocalization, we compared them with prior data from adult zebra finch Area X (Hilliard et al., 2012a; Hilliard et al., 2012b). Our present network captures a point in zebra finch development when birds are actively learning how to improve their songs whereas in adulthood, the learning process has ended and adult songs are 'crystallized'. Contrasts between juvenile and adult networks highlight gene coexpression patterns that change between the two learning states, and inform their molecular underpinnings.

Our previous study in adults found multiple modules in Area X that were correlated to singing crystallized songs. We reasoned that if highly similar coexpression patterns were present in juveniles, then they would likely be unrelated to learning. In this case, the capacity to learn a song might be attributable to other genes and/or the relationships between them. To compare across studies, we built two new, age-specific networks composed of genes common to the two

original networks, then computed gene significance scores for all genes in both networks. We found a remarkable correlation between gene significances to singing in juveniles and adults (Figure 5A), showing that genes in Area X shared similar relationships to singing, whether it be positive, negative, or nonexistent, independent of the animal's age and learning state. The replicated discovery of specific sets of song-production genes across studies and ages speaks to the profound effect that singing behavior has on gene transcription profiles within the song-dedicated basal ganglia.

We next calculated module preservation across the two studies, which assesses how well the coexpression relationships between genes persist across ages (Langfelder et al., 2011). We observed strong to very strong relationships between module preservation and correlation to singing, and genes related to singing clustered together independent of age (Figure 5B and C, Supplementary file 4). These results indicate that not only are the relationships between genes and singing consistent across ages but those genes' coexpression patterns are preserved as well. Since singing-driven gene coexpression patterns were similar between juvenile and adult Area X, the capacity to learn vocalizations is not a product of large-scale differences in coexpression of the song production module genes. We therefore looked for any modules that differed between juvenile and adult Area X. We found that the green, greenyellow and darkred learning-related modules that were significantly correlated to tutor similarity in juveniles were poorly preserved in adult Area X (Figure 5B and C, Supplementary file 4). Irrespective of preservation between juvenile and adult Area X, the genes in song production and learning-related modules were similarly activated by singing (Figure 5D, top row) and the ranked gene expression within each module displayed a positive correlation across ages (Figure 5D, middle row). However, only the song production modules showed positive correlations between connectivity in juvenile and

adult Area X (Figure 5D, bottom row). These results attribute the difference between juvenile and adult Area X not to differential expression or altered correlation to behavior, but to differential connectivity in adults of modules that are correlated to tutor similarity in juveniles. Our findings suggest that the capacity to alter vocalizations may not reside in the absolute expression level of a given gene but instead the gene's transcriptional context. For example, FMR1 was poorly connected in the adult network but was positioned as a hub gene in the juvenile network, indicating the gene's importance during a developmental period when vocalizations are being actively modified but not during their maintenance. In general, genes that were positively correlated with learning and/or had high module membership in the green learning-related module had the greatest decrease in connectivity in adulthood (Figure 5—figure supplement 1).

A bioinformatics approach indicates MAPK11 as an entry point to neuromolecular networks for vocal learning

Above we describe two classes of coexpression modules: (1) learning-related modules that are preserved throughout the striatopallidum but present only in juveniles, (2) song production modules that are preserved across age but specific to Area X. Therefore, song production modules and learning-related modules exist simultaneously only in juveniles, and their co-occurrence within Area X may reflect the capacity to dramatically alter vocalizations during sensorimotor learning. Therefore, we hypothesized that interactions between these two modules may drive the vocal learning process.

To test this idea using bioinformatics, we examined any genes linked to FoxP2, whose overexpression drove the broad range of tutor song copying in our animals. The gene with the greatest gene significance to learning was *MAPK11* (Figure 6A and B). Interestingly, in Foxp2

heterozygous knockout mice, *MAPK11* levels increase, supporting the interaction we observed here (Enard et al., 2009). To examine whether *MAPK11* could be a target of FoxP2 in the zebra finch, we scanned the *MAPK11* gene for sequences corresponding to the FoxP2 binding motif from the JASPAR database (see Materials and methods) (Nelson et al., 2013; Mathelier et al., 2016). We found a match with a single base difference beginning 288 base pairs upstream of the zebra finch *MAPK11* transcription start site identified in the RefSeq model (Figure 6C). (Note that the RefSeq model may be incomplete; see *MAPK11* annotation note in Materials and methods). We then used chromatin immunoprecipitation followed by PCR (ChIP-PCR) to test whether or not FoxP2 binds this predicted *MAPK11* regulatory region. Chromatin-immunoprecipitation of FoxP2 enriched a *MAPK11* fragment of the predicted size and encompassing the putative FoxP2 binding site. Moreover, the sequenced fragment contains the FoxP2 binding motif (Figure 6D, Figure 6—figure supplement 1). Taken together, these data suggest that birds overexpressing FoxP2.FL may be limited in their capacity to learn due, at least in part, to FoxP2 regulation of *MAPK11*. In line with this, both the FoxP2.10+ and GFP animals had higher *MAPK11* gene significance scores for tutor similarity than did FoxP2.FL animals (Figure 6A).

A strength of WGCNA is the 'guilt by association' approach whereby genes in close network proximity to a gene of interest become candidates for a role in the same biological processes. With this in mind, we used *MAPK11* as an entry point to pathways related to vocal learning. We first scanned for genes with high topological overlap with *MAPK11* (e.g. the closest network neighbors to *MAPK11*). Many of these genes were well-connected members of the green learning module (Figure 6E). One such gene, *ATF2* (formerly known as *CREB2*), had the fifth highest green intramodular connectivity and third highest whole network connectivity

(Supplementary file 1). ATF2 protein is necessary for proper development of the nervous system (Reimold et al., 1996) and serves a dual purpose in affecting transcription by binding to cAMP response elements and also by acetylating histones H2B and H4 (Bruhat et al., 2007; Kawasaki et al., 2000). Like FMR1, *ATF2* is poorly connected in the adult network (Hilliard et al., 2012a).

While its role in development of the nervous system has been defined, no specific relationship between ATF2 and learned vocalization has been described. In our network, the ATF2 acetylation target histone H2B sorted into the blue song production module, which is strongly and positively correlated to the act of singing (Figure 3B, Supplementary file 1) and acetylation of histone H2B at lysine five has been linked to learning and memory in rat hippocampus (Bousiges et al., 2013). A pathway such as this represents an interaction between a network hub in a learning module (*ATF2*) and a song production module gene (histone H2B) at a developmental time point at which the bird is actively learning its vocalizations.

To generalize this strategy, we used the Search Tool for the Retrieval of Interacting Genes/Proteins (STRING) database (Szklarczyk et al., 2015) to identify additional interactions between learning-related network hubs and song production genes in Area X. We submitted genes from the green, greenyellow, and darkred learning-related modules and the black, blue, darkgreen, orange, and royalblue song production modules, then filtered for cross-module interactions and scaled the confidence scores by the average intramodular connectivity of each gene in the interaction. This yielded a ranked list of interactions between genes positively correlated to learning and those correlated to singing, which was prioritized by weighted confidence score to yield the highest confidence interactions between genes with the greatest network importance (Supplementary file 5). These interactions were plotted as a network with proteins as nodes and interaction scores as edges (Figure 7). This approach allowed us to not

only visualize the confidence in gene interactions but also the local neighborhoods formed by the protein interaction network, emphasizing genes of potentially greater importance in the vocal learning process based on the number of interactions they have.

We ranked interactions by four different metrics designed to emphasize or deemphasize gene significance, intramodular connectivity, and differential connectivity in juveniles vs. adults (see Materials and methods). These metrics provide a basis for selecting protein-protein interactions based on the relationship to the genes and their most strongly correlated behavior, the coexpression network importance of the genes, or the change in connectivity between juvenile and adult birds. In using the latter metric, the decreased connectivity of learning-related genes *ATF2* and *FMR1* in adulthood is accounted for and interactions involving those genes are prioritized. Interactions between *ATF2* and *IRF2*, *DUSP5*, and *FOS* are among the highest scoring interactions using this metric. All such interactions are presented in Supplementary file 5.

Construct-specific networks

In addition to the overall Area X network presented above, we built and compared construct-specific networks from birds injected with the FoxP2.FL expressing virus versus those injected with the FoxP2.10+ expressing virus versus those expressing GFP (Figure 3—figure supplements 1–3). This analysis enabled us to assess the level of construct-driven changes in gene coexpression as well as to test for the presence of the learning-related module in the control birds whose FoxP2 levels were unmanipulated. We quantified module preservation between the FoxP2 networks and the GFP network (Figure 3—figure supplement 4). In both FoxP2 networks, a gradient of module preservation was observed versus the GFP network with both overlapping and significantly different modules observed. Birds in these experimental conditions were

siblings, and in some cases from the same clutch, suggesting that the driving effect of network differences is the construct-specific manipulation. The green learning-related module was well-preserved across the three networks. The strong correlation of this module to learning passed false discovery rate correction in the GFP cohort comprised of only seven birds, indicating that the learning-related coexpression pattern observed in the overall network is also present without FoxP2 manipulation.

Discussion

In this study, we overexpressed FoxP2 isoforms or GFP and thereby created a range of song learning and song variability induction (Figure 2F), ideal for transcriptome profiling and WGCNA. We constructed an overall Area X gene network and discovered modules correlated to singing, learning, and vocal variability. The network properties of these modules revealed strong relationships between gene module membership and the behavior(s) to which the modules were correlated.

To understand how gene coexpression patterns change across the boundary of the sensorimotor critical period for vocal learning, we compared the juvenile Area X overall network constructed here to one previously constructed from adult Area X (Hilliard et al., 2012a). We had competing hypotheses about whether the inability to learn new songs as an adult is resultant of changes to the song production modules observed in juveniles or associated with some other transcriptional change. Module preservation statistics revealed robust preservation of the juvenile Area X song production modules in the adult network, supporting the latter hypothesis. In striking contrast, the densely interconnected green learning-related module observed in juvenile striatopallidum was poorly preserved in adults, indicating that at least part of the learning-related transcriptome is altered by aging. Further, the green learning-related module was strongly

preserved across the construct-specific networks (Figure 3—figure supplements 1–4) and robustly correlated to learning in the GFP network. This latter finding suggests that the coexpression of these genes occurs in non-manipulated birds and is not a byproduct of experimental perturbation of FoxP2 levels.

Because we created networks from VSP of the same animals, we could compare how well the Area X modules were preserved in a similar brain region that is unspecialized for song. As in Hilliard et al. (2012a), Area X song production modules were poorly preserved in VSP in contrast to the strongly preserved green learning-related module. These experiments define juvenile Area X as a nexus wherein the striatopallidal learning-related modules exist in tandem with song production modules. As the brain ages, singing continues to drive transcriptional patterns in Area X but the learning-related patterns are lost (Figure 8A; Figure 8B). Our findings suggest a model for the molecular basis of complex learned vocal behavior as – not specific genes or coexpression modules but rather the spatiotemporal overlap of 'singing' and 'learning' building blocks. Song control nuclei are proposed to have evolved as specializations of pre-existing motor circuitry (Pfenning et al., 2014; Feenders et al., 2008). A similar principle may thus extend across the songbird telencephalon whereby nonspecialized/learning related and specialized/behavior related coexpression patterns converge to permit sensorimotor learning.

Our findings validate prior results in which overexpression of FoxP2.FL prevented practice-induced changes in song variability and impaired song learning. These results support the hypothesis that behavior-linked cycling of FoxP2, rather than its absolute level, is critical for vocal learning. In addition, we uncovered singing-induced vocal invariability as a novel behavioral effect of FoxP2.10+ overexpression. Despite the poor exploration of motor space induced by FoxP2.10+ overexpresssion, these animals learned their tutors' songs well, a finding

seemingly at odds with motor learning theory where broad exploration of motor space is refined through practice before arriving at an 'ideal' precise pattern for execution of the skill (Kaelbling et al., 1996; Wu et al., 2014). A similar phenomenon was observed in a different species of passerine songbird, the Bengalese finch (Lonchura striata domestica), where two hours of UD singing resulted in less variable songs than those sung after two hour of non-singing (Chen et al., 2013). In both species, the inability to induce song variability did not affect vocal learning, suggesting that the ability to have relatively low or high variability states in singing are necessary to properly learn a song regardless of whether those differential variability states precede or follow singing.

WGCNA identified FMR1 as a gene of great importance in a learning module. FMR1 encodes an RNA-binding protein and therefore its levels could have a profound effect on a number of targets in the network (Ascano et al., 2012). FMR1 protein is expressed throughout the zebra finch song control circuit primarily in neurons, and birdsong has been suggested as an interesting model in which to study the gene's function (Winograd and Ceman, 2012; Winograd et al., 2008). Here, we observed a correlative link between FMR1 expression and how well the animal copied its tutor's song, a novel association that could be reasonably hypothesized given the speech and language phenotype associated with FMR1 deficiency in humans. A key strength of WGCNA is the ability to query the network around genes known to be associated with a trait. *FMR1*'s close network neighbors included *ATF2* which has been associated with learning but has no prior link to vocal behavior. Further investigation into the learning-related modules is likely to reveal pathways fundamental to procedurally learned behavior.

To identify those molecules that may interact at this particular developmental time point and brain region, we selected *MAPK11* – a likely FoxP2 target (Enard et al., 2009) and the gene

with the greatest significance to learning – to further investigate as an entry point to the pathways underlying learning behavior. Local neighborhood analysis of *MAPK11* in the coexpression network revealed high topological overlap with many strongly connected members of green learning-related module, including the hub gene *ATF2*. ATF2 is a phosphorylation target of *MAPK11* and part of an evolutionarily-conserved pathway for learning and memory (Guan et al., 2003). This phosphorylation enhances ATF2 histone-acetyltransferase activity (Enslen et al., 1998; Stein et al., 1997). A known enzymatic substrate of ATF2 is histone H2B (Kawasaki et al., 2000), a member of the blue song production module that is positively correlated to singing. To probe for additional protein-protein interactions such as these, we mined the STRING database using song production and learning-related module members, then prioritized the interactions based on the network properties and/or behavioral significance of the input genes. A prioritized list of interactions and a complex network emerged, highlighting genes based on their coexpression network importance and/or the number of protein level interactions in the database (Figure 7, Supplementary file 5).

While there are differences in overall gene expression between the juvenile and adult brain, the context within which genes express, that is, their connectivity, is drastically altered, especially in the learning-related modules. Changes in connectivity are not necessarily indicative of changes in the absolute level of a gene's expression, as evidenced by the comparisons between Area X and VSP (Figure 4D) or juvenile and adult Area X (Figure 5D), where expression levels correlate positively but connectivity does not. These data support the idea that the coexpression patterns, and thereby the genes' connectivity and network importance, contribute to the transition from a state of learning to a state of non-learning.

In using connectivity as a measure of network importance and protein interaction as a measure of functional biological output, the protein interaction landscape underlying learned vocal behavior shifts across the two developmental time points analyzed here. For example, the local interaction network around green module hub *ATF2* (defined as all those neighbors within two steps and with high confidence of protein interaction) is composed of well-connected genes in the learning-related and song production modules (Figure 8C, top). Moreover, the connections to learning-related genes are, themselves, inputs to well-connected network hubs. As the juvenile crosses over into adulthood, the connectivity of many of the learning-related genes, like *ATF2*, dramatically decreases. As part of the same process, the adjacencies between genes in the interaction network shift such that a connection to a learning-related gene is no longer one with a hub (Figure 8C, bottom). This shift in network importance may present a pattern underlying song maintenance rather than song learning, and potentially the closure of the critical period in which the bird can change its song.

To understand the mechanisms underlying the transition between the two learning states, our data highlight the importance of the network position of a gene. To enable vocal plasticity after critical period closure, a goal critically relevant to social and communication disorders, manipulations that coordinate gene expression such that poorly connected genes are reestablished as network hubs are likely required. Tools to accomplish a goal such as this do not yet exist, but the pathways prioritized and presented here provide a framework for teasing out testable components.

In sum, we have described the Area X transcriptome at a developmentally significant point in the vocal learning process and provided context for it in terms of aging and brain region specificity. We suggest numerous coexpression and protein level interactions that our data

indicate are significant to vocal learning. Due to the large amount of data generated by this study, we provide interactive graphics describing the coexpression and protein interaction networks as a supplement to the figures and tables in the manuscript. These, and the compiled descriptive statistics are hosted at (https://www.ibp.ucla.edu/research/white/genenetwork.html). We encourage exploration of these datasets to confirm or refute their validity and to provide the molecule-to-behavior links suggested herein.

Acknowledgments

We thank Jennifer Morales and Maria Truong for their assistance in analyzing song and non-vocal behavior. Insightful comments from three reviewers were provided on prior versions of the manuscript. This work was supported by NIH grant RO1MH07012 (SAW). ZDB received support from the 'Neuroendocrinology, Sex Differences, and Reproduction' training grant 5T32HD007228.

Figures

Figure A1. Overexpression of FoxP2 isoforms.

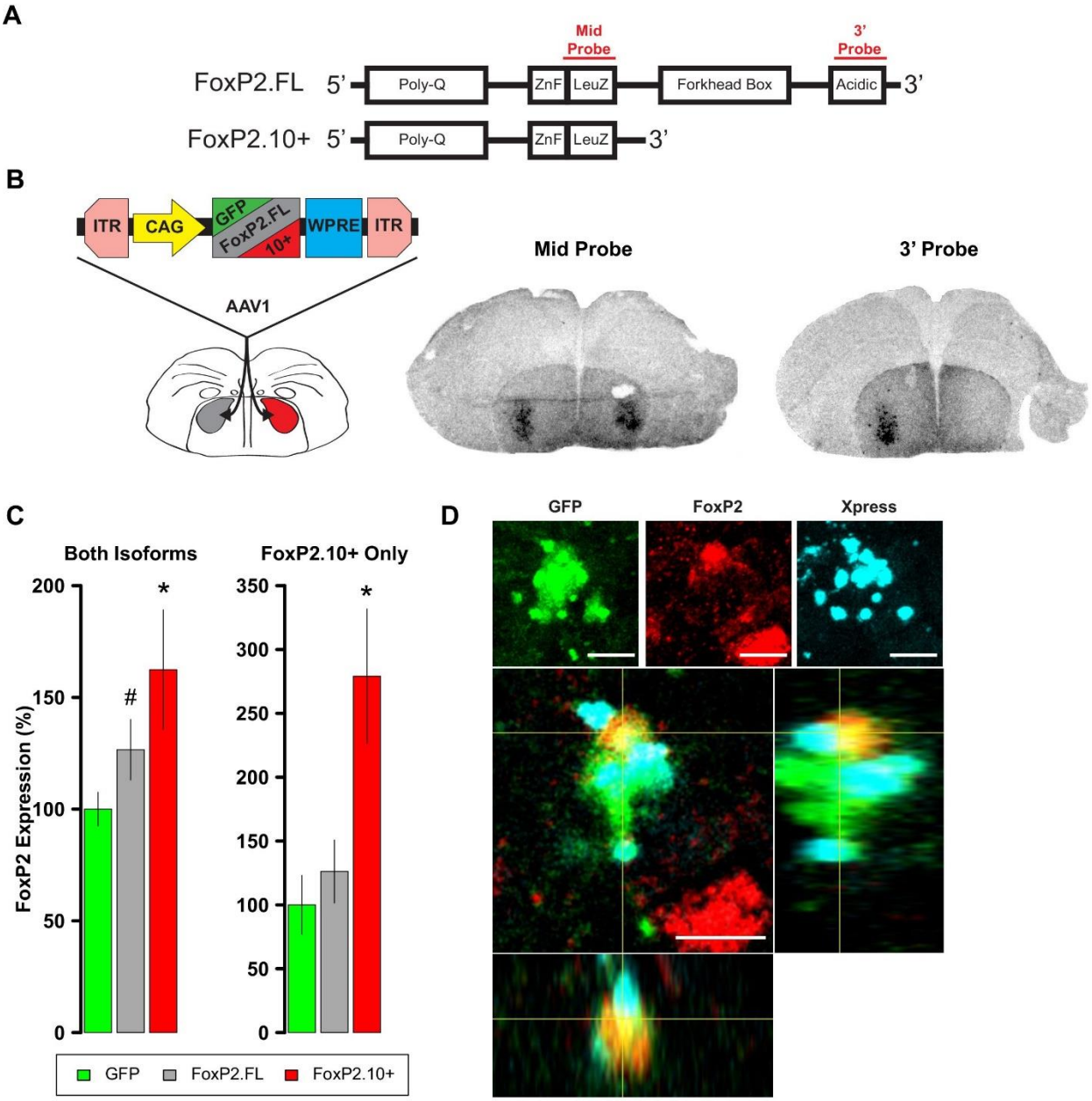

(A) Schematics show full-length (FoxP2.FL) and 10+ (FoxP2.10+) isoforms. Regions whose transcripts were targeted by the complementary riboprobes are shown in red. **(B)** Left panel depicts experimental design to test for isoform-specific expression in vivo. Middle and right images depict two sections from the same female brain. For purposes of validation only, the

bird's right hemisphere (shown on left) was injected with an AAV expressing FoxP2.FL while the left hemisphere was injected with the FoxP2.10+ construct. Two weeks post-injection, robust signals were observed in the striatopallidum of both hemispheres using the mid probe but only in the hemisphere injected with the FoxP2.FL construct using the 3' probe. Signals reflect both the endogenous FoxP2 expression pattern (Teramitsu and White, 2006; Teramitsu et al., 2004; Teramitsu et al., 2010) as well as enhanced levels due to viral-driven expression. **(C)** FoxP2 expression quantified by qRT-PCR in juvenile males that were bilaterally injected with one of the constructs at 35d using primers that identify both isoforms (left graph) or only the FoxP2.10+ isoform (right graph). Using the former primers, enhanced expression is observed in the FoxP2.FL (grey; 126.5 ± 13.53%; n = 6) and FoxP2.10+ (red; 162.4 ± 26.77%; n = 6) groups relative to levels of birds that received the GFP control construct (green; 100 ± 7.54%; n = 7). Using the 'FoxP2.10+ Only' primers, enhanced expression is only observed in the FoxP2.10+ group (red; 279 ± 52.69%; n = 6) vs. the FoxP2.FL (grey; 126.16 ± 24.61%; n = 6) and GFP (green; 100 ± 22.95%; n = 7). Values represent percentage relative to GFP ±SEM. * and # denote p=0.031 and p=0.084, respectively, of an unpaired two-tailed bootstrap test. **(D)** A cell in the zebra finch striatopallidum expressing GFP (indicating viral transduction; green), endogenous FoxP2 as revealed by an antibody directed to the C-terminus (red), and Xpress-FoxP2.10+ revealed by an antibody to the Xpress tag (cyan). The Xpress signal is reminiscent of FoxP2.10+ aggresomes observed by Vernes et al. (Vernes et al., 2006). Orthogonal views of the cell are presented below. Scale bar = 5 µM.

Figure A2. Overexpression of FoxP2 Isoforms affect song learning and/or song variability

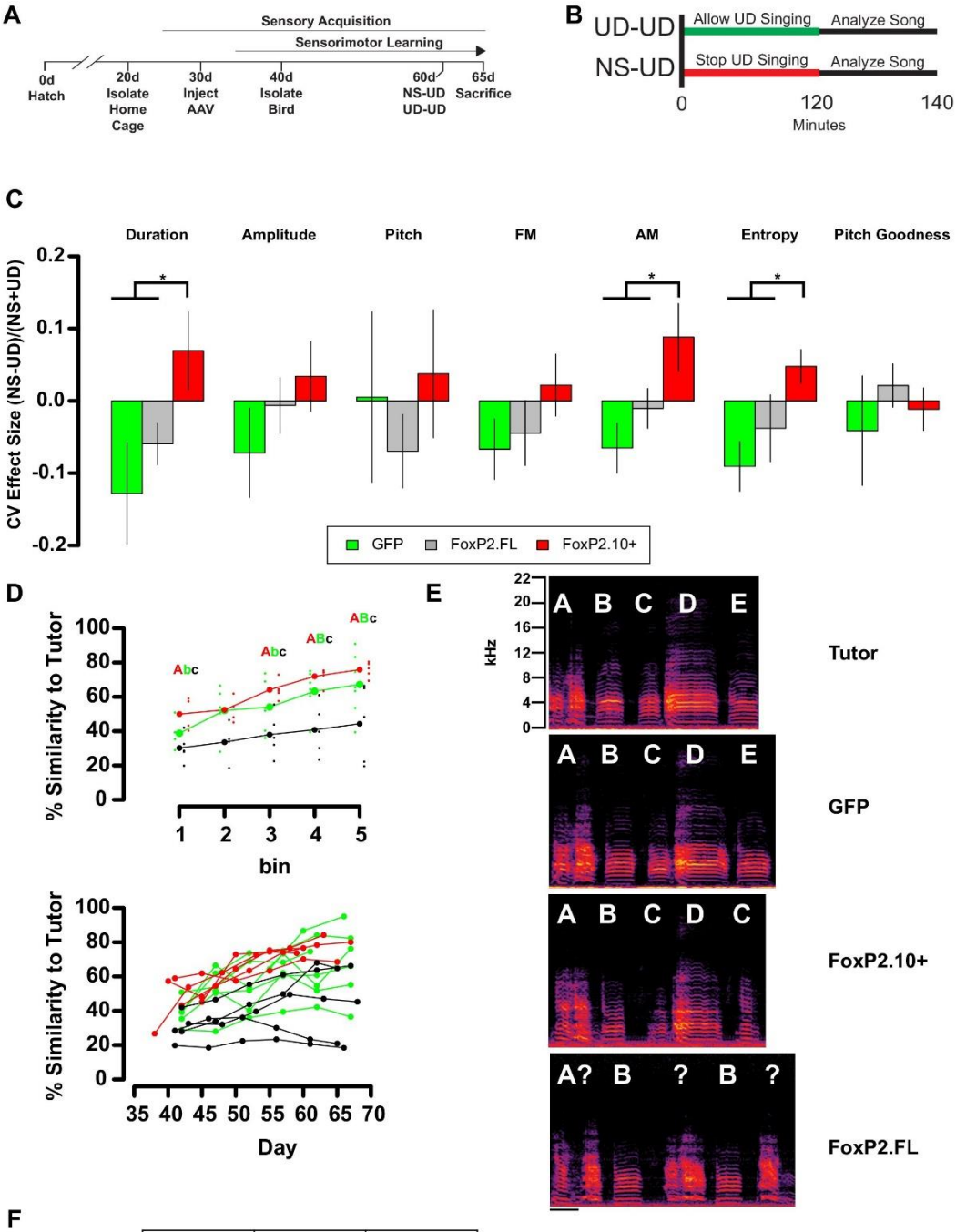

	GFP	FoxP2.FL	FoxP2.10+
Learning	Good	Poor	Good
Variability after UD	Increases	No change	Decreases

(**A**) Timeline of experimental procedures relative to critical periods in song development. (**B**) Schematic illustrates NS-UD or UD-UD experiments performed on adjacent days. (**C**) The effect size of two hours of UD singing on syllable CV was calculated using the formula (NS-UD)/(NS + UD) after an NS-UD, UD-UD experiment performed at ~60d and 61d as in (**B**). Overexpression of FoxP2.FL (grey bars; n = 16 syllables; Duration = −0.059 ± 0.029; AM = −0.010 ± 0.028; Entropy = −0.038 ± 0.04) diminishes singing induced variability relative to that seen in GFP-expressing controls (green bars; n = 9 syllables; Duration = −0.128 ± 0.071; AM = −0.065 ± 0.035; Entropy = −0.091 ± 0.034). In contrast, overexpression of FoxP2.10+ (red bars; n = 13 syllables; Duration = 0.070 ± 0.054; AM = 0.088 ± 0.047; Entropy = 0.048 ± 0.029) leads to a singing-induced state of relative invariability. Values and bar heights represent the average effect size for all syllables within the virus construct group ±SEM. * denotes significant result in one-way ANOVA (Duration: $F(2,35) = 3.95$, $p=0.028$; AM: $F(2,35) = 3.96$, $p=0.028$; Entropy: $F(2,35) = 3.63$, $p=0.037$) and Tukey's HSD post-hoc test ($p<0.05$). (**D**) Learning curves plot the relationship between percentage similarity to tutor as a function of time. Animals overexpressing GFP (green; letter 'B'; n = 7 birds;~65 d similarity = 67.2 ± 6.64%) or FoxP2.10+ (red, letter 'A'; n = 5 birds;~65 d similarity = 75.8 ± 2%) learn significantly better than those overexpressing FoxP2.FL (grey, letter 'C'; n = 5 birds;~65 d similarity = 44.3 ± 10.1%). Values are mean ±SEM. Data are binned by day (top panel; bold points represent group mean and shifted smaller points are individual birds) or by individuals (bottom panel). Significantly different groups tested by one-way ANOVA (Bin 1:~40d $F(2,11) = 6.06$, $p=0.016$; Bin 3:~55d $F(2,13) = 6.04$, $p=0.014$; Bin 4:~60d $F(2,14) = 9.94$, $p=0.002$; Bin 5:~65d $F(2,14) = 4.76$, $p=0.026$) and Tukey HSD post-hoc test ($p<0.05$) are denoted by capital and lowercase

lettering. (**E**) Exemplar motifs of a tutor and three of his 65d pupils, each of which was injected with a different viral construct at 30d. These examples illustrate the percent similarity depicted in panel D. (**F**) Summary of the learning and variability phenotypes observed after virus injection.

Figure A3. WGCNA yields behaviorally relevant modules

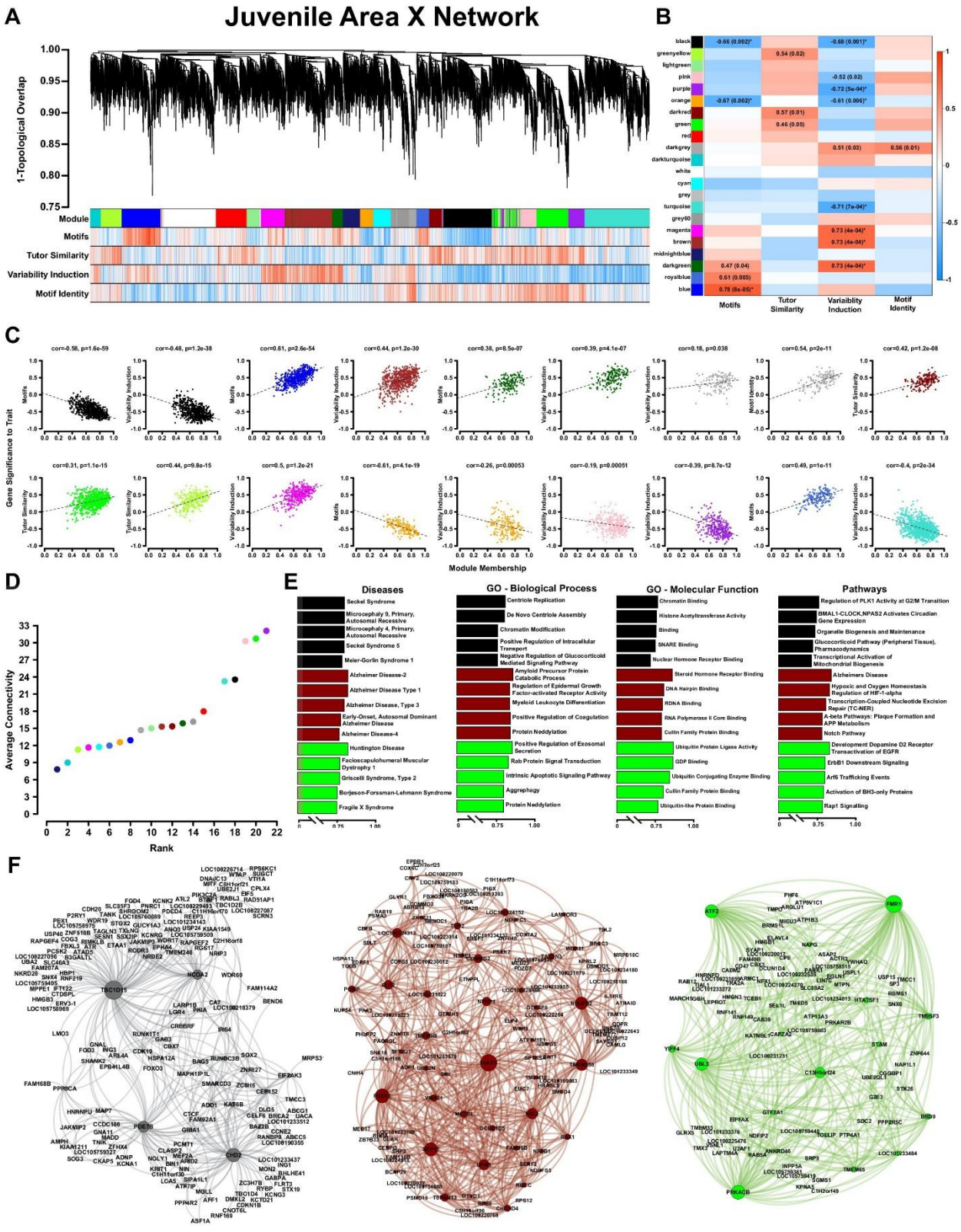

(**A**) Dendrogram (top) illustrates the topological overlap between genes in the juvenile Area X overall network. Modules delineated by automated tree trimming are shown below and are depicted by arbitrary colors. Beneath the color bar, gene significances to the quantified behaviors (number of motifs sung, tutor similarity, acute variability changes, and overall variability; see Results) are indicated by a heatmap wherein red indicates a positive correlation and blue indicates a negative correlation (see B for scale). (**B**) Correlations between module eigengenes and each behavior are presented as a heatmap. The Pearson's ρ and, in parentheses, Student's asymptotic p-values for modules where $p \leq 0.05$ are displayed. P-values are uncorrected for multiple hypothesis testing but those that pass FDR correction at $p \leq 0.05$ are denoted by * (See 'Correlation of behavior to gene expression' in Materials and methods). (**C**) For all significant module-trait correlations, the relationship between gene significance and module membership is plotted for each gene in the module. Dashed lines represent the linear regression and the Pearson's ρ ('cor') and p-value as determined by Fisher's z-transformation are indicated above each plot. (**D**) The average whole network connectivity (kTotal) within each module reveals that the purple, green, and pink modules are composed of the most strongly connected genes in the network. (**E**) Term significances for the black, darkred, and green modules are indicated for disease, gene ontology biological process and molecular function, as well as for pathways for categories annotated as 'neuronal' in the GeneCards GeneAnalytics software. (**F**) Network plots of the modules presented in panel E where nodes represent genes scaled by the node's intramodular connectivity and edge width displays the topological overlap between genes.

Figure A4. Juvenile Area X singing related gene coexpression patterns are not preserved in juvenile VSP

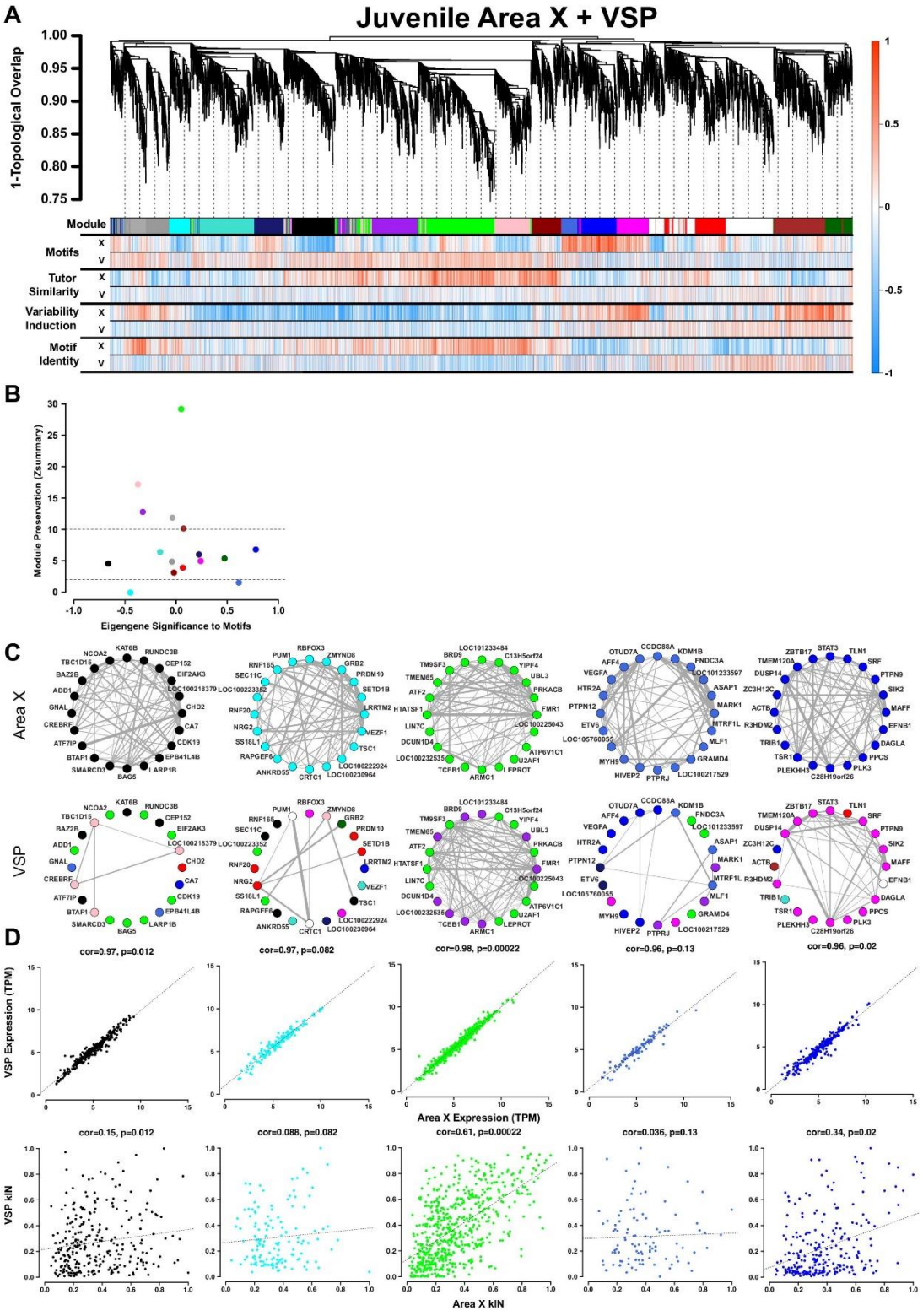

(**A**) Dendrogram (top) displays the topological overlap in Area X between genes common to both juvenile Area X and VSP networks. Beneath, the module assignments and the gene significances for each gene as calculated using expression from VSP ('V') or Area X ('X') for all behaviors are quantified as in Figure 3A. Module colors are consistent with those presented in Figure 3. (**B**) Module preservation (Zsummary) for all modules that were present in both Area X and VSP displayed as a function of module eigengene correlation to motifs. Lower and upper dashed horizontal lines indicate thresholds for low and high preservation, respectively. (**C**) Circle plots display the adjacencies between the 20 most well-connected genes in the Area X black, cyan, green, royalblue, and blue modules. The adjacency between genes is indicated by edge thickness. Genes grouped together in the black, cyan, royalblue, and blue song modules in Area X have numerous and strong connections. Those connections are weakened or nonexistent in VSP such that genes sort into different modules in VSP. In contrast, the green learning-related module genes maintain their common grouping and connections in VSP. (**D**) Raw gene expression is tightly correlated between Area X and VSP for the genes in the black, cyan, green, royalblue, and blue modules (top). Only the intramodular connectivity of the genes in the green learning-related module is correlated between Area X and VSP (bottom). Dashed lines represent the linear regression.

Figure A5. Area X song production but not learning-related modules are preserved into adulthood

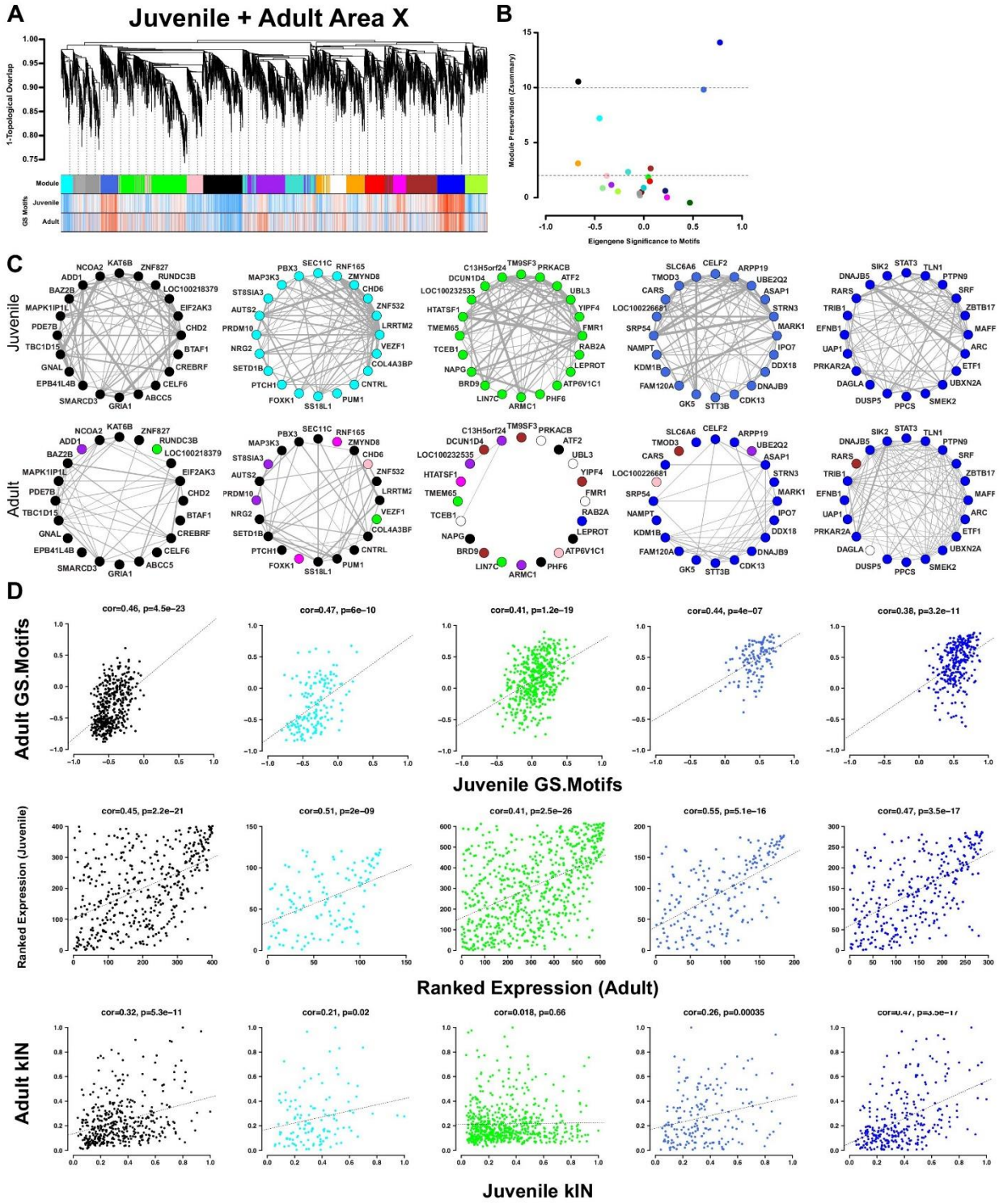

(**A**) Dendrogram (top) displays the topological overlap in juvenile Area X between genes

common to both juvenile and adult Area X networks. The module assignments and the gene significances to motifs in juveniles and adults are presented below. Module colors are consistent with those presented in Figure 3. (**B**) Module preservation (Zsummary) for all modules that were present in both juvenile and adult Area X displayed as a function of ME correlation to motifs. Lower and upper dashed horizontal lines indicate thresholds for low and high preservation, respectively. (**C**) Circle plots display the adjacencies between the 20 most well-connected genes in the juvenile Area X black, cyan, green, royalblue, and blue modules. The adjacency between genes are indicated by edge thickness. Genes grouped together in the black, cyan, royalblue, and blue song modules in Area X have numerous and strong connections that are mostly maintained in adulthood. The densely interconnected green learning-related module genes found in juveniles do not maintain these relationships in adulthood. (**D**) Strong positive correlations between gene significance to motifs exist for all modules (top row). Ranked expression values for the genes in each module also show positive correlation (middle row). Intramodular connectivity is more positively correlated between ages for the black, cyan, royalblue, and blue song production modules than for the green learning-related module (bottom row).

Figure A6. Gene significance and network position implicate *MAPK11* as a molecular entry point to vocal learning mechanisms

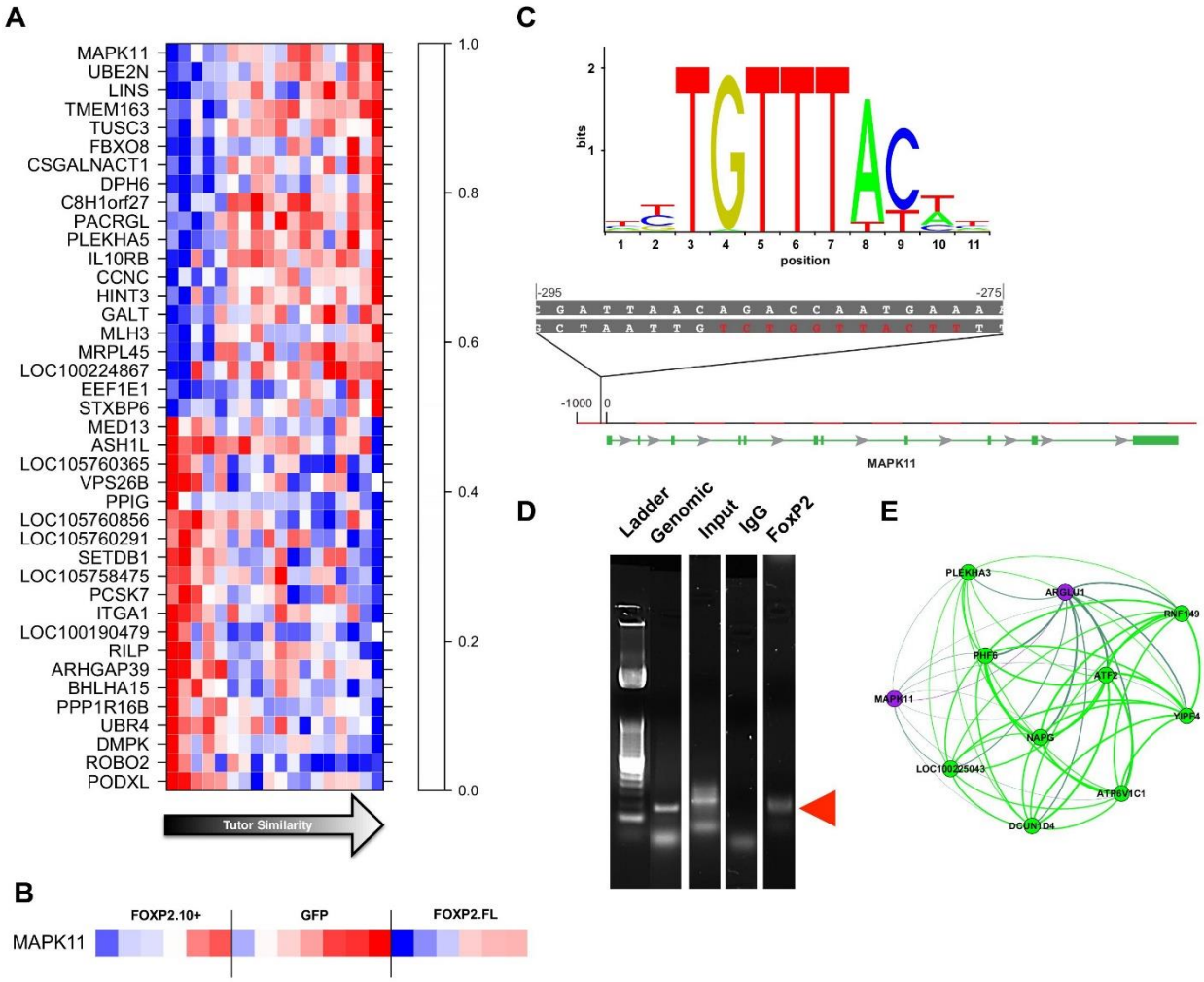

(**A**) The 20 genes with the highest to lowest gene significances to tutor similarity (sorted from top to bottom) are shown. Each column represents a bird and columns are sorted in order of increasing tutor similarity from left to right. Gene expression is scaled such the highest and lowest expression across samples have the brightest shade of red or blue, respectively. (**B**) Expression of *MAPK11* is replotted, here separated by virus group and then sorted by increasing tutor percentage similarity. (**C**) The FoxP2 binding sequence as annotated by the JASPAR database (top) and a potential binding site found in the *MAPK11* 'promoter'. (**D**) Amplification

of genomic DNA ('Genomic') with primers for a region of the *MAPK11* 'promoter' that contains a putative FoxP2 binding site enrich a fragment of predicted size (red arrowhead) in the pull-down lane (FoxP2) but not the control (IgG) lane. (**E**) *MAPK11* and its 10 closest network neighbors, including green learning-related module members and hub gene *ATF2*, as defined by topological overlap.

Figure A7. Protein-level interactions between song production and learning-related module genes in juvenile Area X

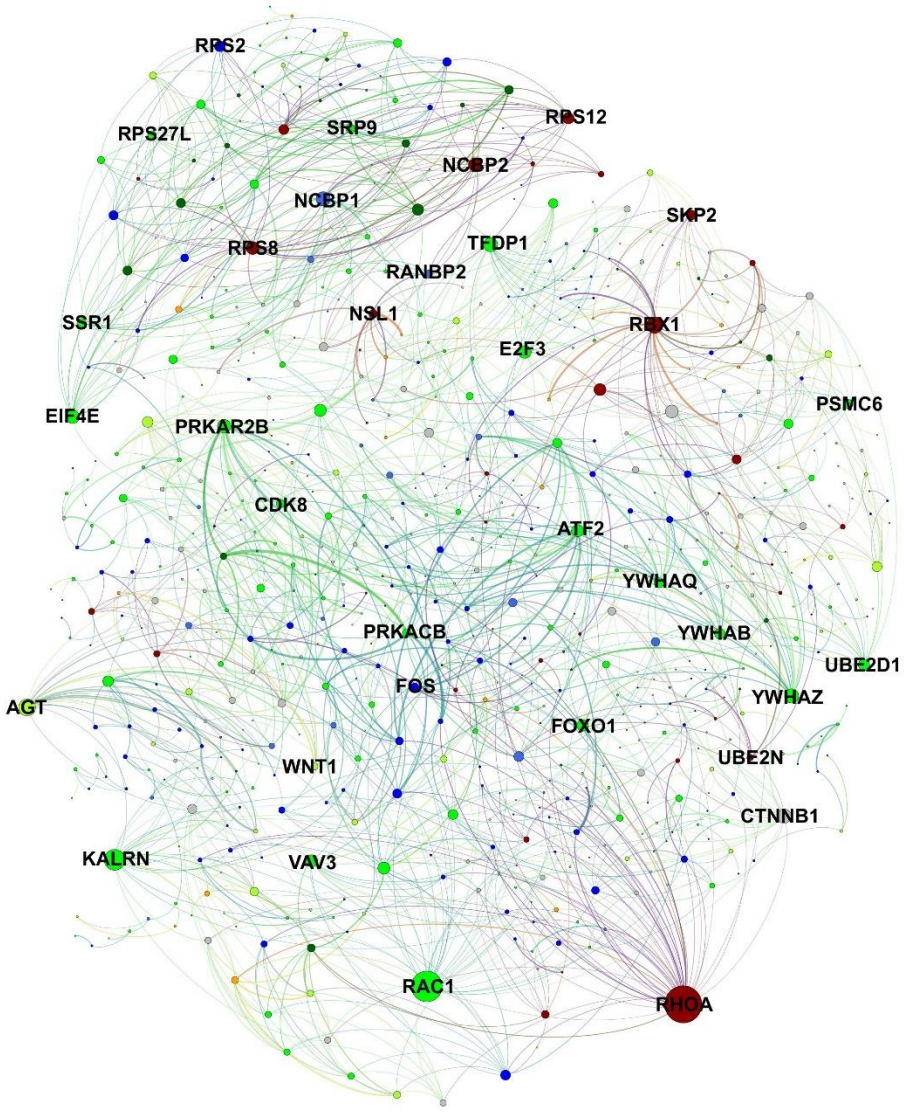

A protein interaction network plot using the STRING database between genes in learning-related (darkred, green, greenyellow) and song production (black, blue, darkgreen, orange, royalblue) modules. Nodes are scaled by number of connections. Edge width is determined by scaling the STRING protein interaction confidence score for the two nodes by the product of each node's intramodular connectivity. Interactions within learning or song production modules are omitted for clarity.

Figure A8. Changes in vocal plasticity state between juvenile and adult birds

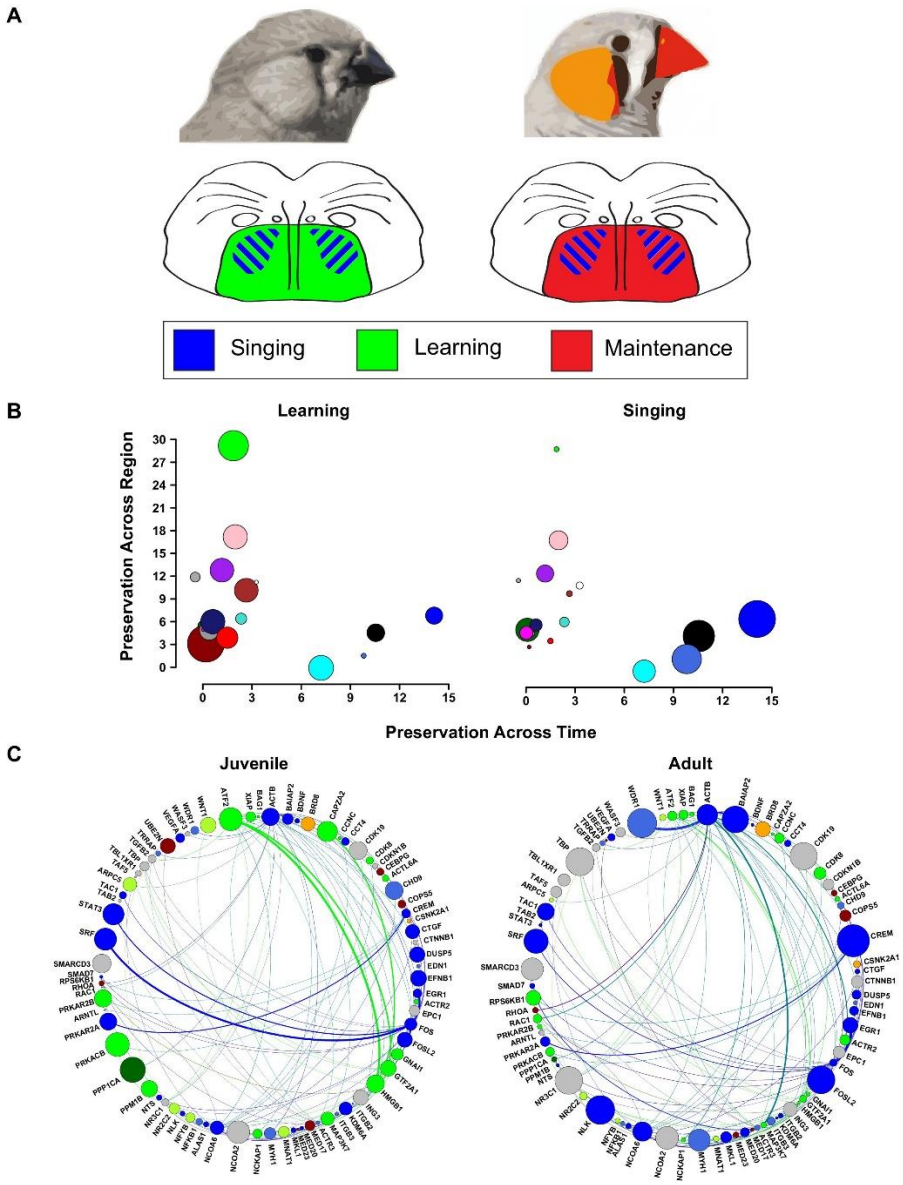

(**A**) Schematics depict the juvenile straitopallidum (left) in a 'plastic' state in which genes in learning-related modules (green) are densely interconnected and of high importance in the network. Simultaneously, singing driven gene coexpression patterns (blue) occur in Area X. In the adult striatopallidum (right), song production modules (blue) exist as they do in juveniles, but the learning-related modules do not and are replaced by coexpression patterns that presumably underlie the maintenance of song (red). (**B**) Area X modules in the juvenile brain are plotted to emphasize their preservation in adult Area X (x-axis) and juvenile VSP (y-axis). Points representing the module colors are scaled by the module's absolute correlation to learning (left) or the absolute correlation to singing (right), emphasizing the preservation of singing coexpression patterns into adulthood and learning coexpression patterns in the juvenile striatopallidum. (**C**) Genes in song production or learning-related modules that are within two steps of *ATF2* in the high-confidence protein interaction network are shown. Nodes are scaled by intramodular connectivity in juveniles (left) or adults (right) with edge width indicative of adjacency between genes in the coexpression network. The change in coexpression patterns across age groups causes decreased connectivity of many learning-related genes, driving an alteration in the network's landscape which may underlie the transition from song learning to song maintenance.

Appendix References

[1] Arriaga G, Zhou EP, Jarvis ED. 2012. Of mice, birds, and men: the mouse ultrasonic song system has somefeatures similar to humans and song-learning birds. PLoS One 7:e46610. DOI: https://doi.org/10.1371/journal.pone.0046610, PMID: 23071596

[2] Ascano M, Mukherjee N, Bandaru P, Miller JB, Nusbaum JD, Corcoran DL, Langlois C, Munschauer M, Dewell S, Hafner M, Williams Z, Ohler U, Tuschl T. 2012. FMRP targets distinct mRNA sequence elements to regulate protein expression. Nature 492:382–386. DOI: https://doi.org/10.1038/nature11737, PMID: 23235829

[3] Barrett HC. 2012. A hierarchical model of the evolution of human brain specializations. PNAS 109 Suppl 1:10733–10740. DOI: https://doi.org/10.1073/pnas.1201898109, PMID: 22723350

[4] Ben-Ari Fuchs S, Lieder I, Stelzer G, Mazor Y, Buzhor E, Kaplan S, Bogoch Y, Plaschkes I, Shitrit A, Rappaport N, Kohn A, Edgar R, Shenhav L, Safran M, Lancet D, Guan-Golan Y, Warshawsky D, Shtrichman R. 2016. GeneAnalytics: An integrative gene set analysis tool for next generation sequencing, rnaseq and microarray data. OMICS: A Journal of Integrative Biology 20:139–151. DOI: https://doi.org/10.1089/omi.2015.0168, PMID: 26983021

[5] Bousiges O, Neidl R, Majchrzak M, Muller MA, Barbelivien A, Pereira de Vasconcelos A, Schneider A, Loeffler JP, Cassel JC, Boutillier AL. 2013. Detection of histone acetylation levels in the dorsal hippocampus reveals early tagging on specific residues of H2B and H4 histones in response to learning. PLoS One 8:e57816. DOI: https://doi.org/10.1371/journal.pone.0057816, PMID: 23469244

[6] Bruce HA, Margolis RL. 2002. FOXP2: novel exons, splice variants, and CAG repeat length stability. Human Genetics 111:136–144. DOI: https://doi.org/10.1007/s00439-002-0768-5, PMID: 12189486

[7] Bruhat A, Chérasse Y, Maurin AC, Breitwieser W, Parry L, Deval C, Jones N, Jousse C, Fafournoux P. 2007. ATF2 is required for amino acid-regulated transcription by orchestrating specific histone acetylation. Nucleic Acids Research 35:1312–1321. DOI: https://doi.org/10.1093/nar/gkm038, PMID: 17267404

[8] Burkett ZD, Day NF, Peñagarikano O, Geschwind DH, White SA. 2015. VoICE: A semi-automated pipeline for standardizing vocal analysis across models. Scientific Reports 5:10237. DOI: https://doi.org/10.1038/srep10237, PMID: 26018425

[9] Castellucci GA, McGinley MJ, McCormick DA. 2016. Knockout of Foxp2 disrupts vocal development in mice. Scientific Reports 6:23305. DOI: ttps://doi.org/10.1038/srep23305, PMID: 26980647

[10] Chabout J, Sarkar A, Patel SR, Radden T, Dunson DB, Fisher SE, Jarvis ED. 2016. A Foxp2 Mutation Implicated in Human Speech Deficits Alters Sequencing of Ultrasonic Vocalizations in Adult Male Mice. Frontiers in Behavioral Neuroscience 10:197. DOI: https://doi.org/10.3389/fnbeh.2016.00197, PMID: 27812326

[11] Chen Q, Heston JB, Burkett ZD, White SA. 2013. Expression analysis of the speech-r elated genes FoxP1 and FoxP2 and their relation to singing behavior in two songbird species. Journal of Experimental Biology 216:3682–3692. DOI: https://doi.org/10.1242/jeb.085886, PMID: 24006346

[12] Clark KL, Halay ED, Lai E, Burley SK. 1993. Co-crystal structure of the HNF-3/fork head DNA-recognition motif resembles histone H5. Nature 364:412–420. DOI: https://doi.org/10.1038/364412a0, PMID: 8332212

[13] Dobin A, Davis CA, Schlesinger F, Drenkow J, Zaleski C, Jha S, Batut P, Chaisson M, Gingeras TR. 2013. STAR: ultrafast universal RNA-seq aligner. Bioinformatics 29:15–21. DOI: https://doi.org/10.1093/bioinformatics/bts635, PMID: 23104886

[14] Dong J, Horvath S. 2007. Understanding network concepts in modules. BMC Systems Biology 1:24. DOI: https://doi.org/10.1186/1752-0509-1-24, PMID: 17547772

[15] Doupe AJ, Kuhl PK. 1999. Birdsong and human speech: common themes and mechanisms. Annual Review of Neuroscience 22:567–631. DOI: https://doi.org/10.1146/annurev.neuro.22.1.567, PMID: 10202549

[16] Dunn AM, Zann RA. 1996. Undirected song in wild zebra finch flocks: Contexts and effects of mate removal. Ethology 102:529–539. DOI: https://doi.org/10.1111/j.1439-0310.1996.tb01145.x

[17] Enard W, Gehre S, Hammerschmidt K, Hoülter SM, Blass T, Somel M, Brückner MK, Schreiweis C, Winter C, Sohr R, Becker L, Wiebe V, Nickel B, Giger T, Müller U, Groszer M, Adler T, Aguilar A, Bolle I, Calzada-Wack J, et al. 2009. A humanized version of Foxp2 affects cortico-basal ganglia circuits in mice. Cell 137:961–971. DOI: https://doi.org/10.1016/j.cell.2009.03.041, PMID: 19490899

[18] Enslen H, Raingeaud J, Davis RJ. 1998. Selective activation of p38 mitogen-activated protein (MAP) kinaseb isoforms by the MAP kinase kinases MKK3 and MKK6. Journal of Biological Chemistry 273:1741–1748. DOI: https://doi.org/10.1074/jbc.273.3.1741, PMID: 9430721

[19] Feenders G, Liedvogel M, Rivas M, Zapka M, Horita H, Hara E, Wada K, Mouritsen H, Jarvis ED. 2008. Molecular mapping of movement-associated areas in the avian brain: a motor theory for vocal learning origin. PLoS One 3:e1768–27. DOI: https://doi.org/10.1371/journal.pone.0001768, PMID: 18335043

[20] Guan Z, Kim JH, Lomvardas S, Holick K, Xu S, Kandel ER, Schwartz JH. 2003. p38 MAP kinase mediates both short-term and long-term synaptic depression in aplysia. Journal of Neuroscience 23:7317–7325. PMID: 12917365

[21] Haesler S, Rochefort C, Georgi B, Licznerski P, Osten P, Scharff C. 2007. Incomplete and inaccurate vocal imitation after knockdown of FoxP2 in songbird basal ganglia nucleus Area X. PLoS Biology 5:e321. DOI: https://doi.org/10.1371/journal.pbio.0050321, PMID: 18052609

[22] Hall MF. 1962. Evolutionary aspects of estrildid song. Symposia of the Zoological Society of London 8:37–55.

[23] Heston JB, White SA. 2015. Behavior-linked FoxP2 regulation enables zebra finch vocal learning. Journal of Neuroscience 35:2885–2894. DOI: https://doi.org/10.1523/JNEUROSCI.3715-14.2015, PMID: 25698728

[24] Hilliard AT, Miller JE, Fraley ER, Horvath S, White SA. 2012a. Molecular microcircuitry underlies functional specification in a basal ganglia circuit dedicated to vocal learning. Neuron 73:537–552. DOI: https://doi.org/10.1016/j.neuron.2012.01.005, PMID: 22325205

[25] Hilliard AT, Miller JE, Fraley ER, Horvath S, White SA. 2012b. Data from: Weighted gene co-expression network analysis on microarray data from subregions of zebra finch (Taeniopygia guttata) basal ganglia. Identifier: Publicly Available at the NCBI Gene Expression Omnibus (Accession No GSE34819).

[26] Horvath S. 2011. Weighted Network Analysis. New York: Springer Science & Business Media. DOI: https://doi.org/10.1007/978-1-4419-8819-5

[27] Immelmann K. 1962. Beiträge zu einer vergleichenden Biologie australischer Prachtfinken (Spermestidae). Zool Jb Sys Bd:1–96.

[28] Jacobs EC, Arnold AP, Campagnoni AT. 1999. Developmental regulation of the distribution of aromatase- and estrogen-receptor- mRNA-expressing cells in the zebra finch brain. Developmental Neuroscience 21:453–472. DOI: https://doi.org/10.1159/000017413, PMID: 10640864

[29] Jürgens U. 2002. Neural pathways underlying vocal control. Neuroscience & Biobehavioral Reviews 26:235–258. DOI: https://doi.org/10.1016/S0149-7634(01)00068-9, PMID: 11856561

[30] Kaelbling LP, Littman ML, Moore AW. 1996. Reinforcement learning: A survey. The Journal of Artificial Intelligence Research 4:237–285.

[31] Kawasaki H, Schiltz L, Chiu R, Itakura K, Taira K, Nakatani Y, Yokoyama KK. 2000. ATF-2 has intrinsic histone acetyltransferase activity which is modulated by

phosphorylation. Nature 405:195–200. DOI: https://doi.org/10.1038/35012097, PMID: 10821277

[32] Lai CS, Fisher SE, Hurst JA, Vargha-Khadem F, Monaco AP. 2001. A forkhead-domain gene is mutated in a severe speech and language disorder. Nature 413:519–523. DOI: https://doi.org/10.1038/35097076, PMID: 11586359

[33] Langfelder P, Horvath S. 2008. WGCNA: an R package for weighted correlation network analysis. BMC Bioinformatics 9:559. DOI: https://doi.org/10.1186/1471-2105-9-559, PMID: 19114008

[34] Langfelder P, Luo R, Oldham MC, Horvath S. 2011. Is my network module preserved and reproducible? PLoS Computational Biology 7:e1001057. DOI: https://doi.org/10.1371/journal.pcbi.1001057, PMID: 21283776

[35] Lemon RN. 2008. Descending pathways in motor control. Annual Review of Neuroscience 31:195–218. DOI: https://doi.org/10.1146/annurev.neuro.31.060407.125547, PMID: 18558853

[36] Liao Y, Smyth GK, Shi W. 2013. The Subread aligner: fast, accurate and scalable read mapping by seed-and-vote. Nucleic Acids Research 41:e108–8. DOI: https://doi.org/10.1093/nar/gkt214, PMID: 23558742

[37] Liao Y, Smyth GK, Shi W. 2014. featureCounts: an efficient general purpose program for assigning sequence reads to genomic features. Bioinformatics 30:923–930. DOI: https://doi.org/10.1093/bioinformatics/btt656, PMID: 24227677

[38] Livak KJ, Schmittgen TD. 2001. Analysis of relative gene expression data using real-time quantitative PCR and the 2(-Delta Delta C(T)) Method. Methods 25:402–408. DOI: https://doi.org/10.1006/meth.2001.1262, PMID: 11846609

[39] Marcus GF, Fisher SE. 2003. FOXP2 in focus: what can genes tell us about speech and language? Trends in Cognitive Sciences 7:257–262. DOI: https://doi.org/10.1016/S1364-6613(03)00104-9, PMID: 12804692

[40] Mathelier A, Fornes O, Arenillas DJ, Chen C-Y, Denay G, Lee J, Shi W, Shyr C, Tan G, Worsley-Hunt R, Zhang AW, Parcy F, Lenhard B, Sandelin A, Wasserman WW. J. 2016. a major expansion and update of the open-access database of transcription factor binding profiles. Nucleic Acids Research 2016:D110–115 . DOI: https://doi.org/10.1093/nar/gkv1176

[41] Miller JE, Spiteri E, Condro MC, Dosumu-Johnson RT, Geschwind DH, White SA. 2008. Birdsong decreases protein levels of FoxP2, a molecule required for human speech. Journal of Neurophysiology 100:2015–2025. DOI: https://doi.org/10.1152/jn.90415.2008, PMID: 18701760

[42] Miller JE, Hilliard AT, White SA. 2010. Song practice promotes acute vocal variability at a key stage of sensorimotor learning. PLoS One 5:e8592. DOI: https://doi.org/10.1371/journal.pone.0008592, PMID: 20066039

[43] Miller JE, Hafzalla GW, Burkett ZD, Fox CM, White SA. 2015. Reduced vocal variability in a zebra finch model of dopamine depletion: implications for Parkinson disease. Physiological Reports 3:e12599–9. DOI: https://doi.org/10.14814/phy2.12599, PMID: 26564062

[44] Nelson CS, Fuller CK, Fordyce PM, Greninger AL, Li H, DeRisi JL. 2013. Microfluidic affinity and ChIP-seq analyses converge on a conserved FOXP2-binding motif in chimp and human, which enables the detection of evolutionarily novel targets. Nucleic Acids Research 41:5991–6004. DOI: https://doi.org/10.1093/nar/gkt259, PMID: 23625967

[45] Neve RL, Neve KA, Nestler EJ, Carlezon WA. 2005. Use of herpes virus amplicon vectors to study brain disorders. BioTechniques 39:381–391. DOI: https://doi.org/10.2144/05393PS01, PMID: 16206910

[46] Oakley TH, Rivera AS. 2008. Genomics and the evolutionary origins of nervous system complexity. Current Opinion in Genetics & Development 18:479–492. DOI: https://doi.org/10.1016/j.gde.2008.12.002, PMID: 19152785

[47] Olias P, Adam I, Meyer A, Scharff C, Gruber AD. 2014. Reference genes for quantitative gene expression studies in multiple avian species. PLoS One 9:e99678. DOI: https://doi.org/10.1371/journal.pone.0099678, PMID: 24926893

[48] Person AL, Gale SD, Farries MA, Perkel DJ. 2008. Organization of the songbird basal ganglia, including area X. The Journal of Comparative Neurology 508:840–866. DOI: https://doi.org/10.1002/cne.21699, PMID: 18398825

[49] Petkov CI, Jarvis ED, Birds JED. 2012. Birds, primates, and spoken language origins: behavioral phenotypes and neurobiological substrates. Frontiers in Evolutionary Neuroscience 4:12. DOI: https://doi.org/10.3389/fnevo.2012.00012, PMID: 22912615

[50] Pfenning AR, Hara E, Whitney O, Rivas MV, Wang R, Roulhac PL, Howard JT, Wirthlin M, Lovell PV, Ganapathy G, Mouncastle J, Moseley MA, Thompson JW, Soderblom EJ, Iriki A, Kato M, Gilbert MT, Zhang G, Bakken T, Bongaarts A, et al. 2014. Convergent transcriptional specializations in the brains of humans and song-learning birds. Science 346:1256846–6. DOI: https://doi.org/10.1126/science.1256846, PMID: 25504733

[51] Reimold AM, Grusby MJ, Kosaras B, Fries JW, Mori R, Maniwa S, Clauss IM, Collins T, Sidman RL, Glimcher MJ, Glimcher LH. 1996. Chondrodysplasia and neurological abnormalities in ATF-2-deficient mice. Nature 379:262–265. DOI: https://doi.org/10.1038/379262a0, PMID: 8538792

[52] Reiner A, Laverghetta AV, Meade CA, Cuthbertson SL, Bottjer SW. 2004. An immunohistochemical and pathway tracing study of the striatopallidal organization of area X in the male zebra finch. The Journal of Comparative Neurology 469:239–261. DOI: https://doi.org/10.1002/cne.11012, PMID: 14694537

[53] Schneider CA, Rasband WS, Eliceiri KW. 2012. NIH Image to ImageJ: 25 years of image analysis. Nature Methods 9:671–675. DOI: https://doi.org/10.1038/nmeth.2089, PMID: 22930834

[54] Stein B, Yang MX, Young DB, Janknecht R, Hunter T, Murray BW, Barbosa MS. 1997. p38-2, a novel mitogen-activated protein kinase with distinct properties. Journal of Biological Chemistry 272:19509–19517. DOI: https://doi.org/10.1074/jbc.272.31.19509, PMID: 9235954

[55] Szklarczyk D, Franceschini A, Wyder S, Forslund K, Heller D, Huerta-Cepas J, Simonovic M, Roth A, Santos A, Tsafou KP, Kuhn M, Bork P, Jensen LJ, von Mering C. 2015. STRING v10: protein-protein interaction networks, integrated over the tree of life. Nucleic Acids Research 43:D447–D452. DOI: https://doi.org/10.1093/nar/gku1003, PMID: 25352553

[56] Tchernichovski O, Nottebohm F, Ho CE, Pesaran B, Mitra PP. 2000. A procedure for an automated measurement of song similarity. Animal Behaviour 59:1167–1176. DOI: https://doi.org/10.1006/anbe.1999.1416, PMID: 10877896

[57] Teramitsu I, Kudo LC, London SE, Geschwind DH, White SA. 2004. Parallel FoxP1 and FoxP2 expression in songbird and human brain predicts functional interaction. Journal of Neuroscience 24:3152–3163. DOI: https://doi.org/10.1523/JNEUROSCI.5589-03.2004, PMID: 15056695

[58] Teramitsu I, White SA. 2006. FoxP2 regulation during undirected singing in adult songbirds. Journal of Neuroscience 26:7390–7394. DOI: https://doi.org/10.1523/JNEUROSCI.1662-06.2006, PMID: 16837586

[59] Teramitsu I, Poopatanapong A, Torrisi S, White SA. 2010. Striatal FoxP2 is actively regulated during songbird sensorimotor learning. PLoS One 5:e8548. DOI: https://doi.org/10.1371/journal.pone.0008548, PMID: 20062527

[60] Thompson CK, Schwabe F, Schoof A, Mendoza E, Gampe J, Rochefort C, Scharff C. 2013. Young and intense: FoxP2 immunoreactivity in Area X varies with age, song stereotypy, and singing in male zebra finches. Frontiers in Neural Circuits 7:24. DOI: https://doi.org/10.3389/fncir.2013.00024, PMID: 23450800

[61] Vargha-Khadem F, Watkins KE, Price CJ, Ashburner J, Alcock KJ, Connelly A, Frackowiak RS, Friston KJ, Pembrey ME, Mishkin M, Gadian DG, Passingham RE. 1998. Neural basis of an inherited speech and language disorder. PNAS 95:12695–12700. DOI: https://doi.org/10.1073/pnas.95.21.12695, PMID: 9770548

[62] Vernes SC, Nicod J, Elahi FM, Coventry JA, Kenny N, Coupe AM, Bird LE, Davies KE, Fisher SE. 2006. Functional genetic analysis of mutations implicated in a human speech and language disorder. Human Molecular Genetics 15:3154–3167. DOI: https://doi.org/10.1093/hmg/ddl392, PMID: 16984964

[63] Winograd C, Clayton D, Ceman S. 2008. Expression of fragile X mental retardation protein within the vocal control system of developing and adult male zebra finches. Neuroscience 157:132–142. DOI: https://doi.org/10.1016/j.neuroscience.2008.09.005, PMID: 18835331

[64] Winograd C, Ceman S. 2012. Exploring the zebra finch Taeniopygia guttata as a novel animal model for the speech-language deficit of fragile X syndrome. Results and Problems in Cell Differentiation 54:181–197. DOI: https://doi.org/10.1007/978-3-642-21649-7_10, PMID: 22009353

[65] Wu HG, Miyamoto YR, Gonzalez Castro LN, O¨ lveczky BP, Smith MA. 2014. Temporal structure of motor variability is dynamically regulated and predicts motor learning ability. Nature Neuroscience 17:312–321. DOI: https://doi.org/10.1038/nn.3616, PMID: 24413700

[66] Ye J, Coulouris G, Zaretskaya I, Cutcutache I, Rozen S, Madden TL. 2012. Primer-BLAST: a tool to design target-specific primers for polymerase chain reaction. BMC Bioinformatics 13:134. DOI: https://doi.org/10.1186/1471-2105-13-134, PMID: 22708584

[67] Yip AM, Horvath S. 2007. Gene network interconnectedness and the generalized topological overlap measure. BMC Bioinformatics 8:22. DOI: https://doi.org/10.1186/1471-2105-8-22, PMID: 17250769

[68] Zhang B, Horvath S. 2005. A general framework for weighted gene co-expression network analysis. Statistical Applications in Genetics and Molecular Biology 4:Article17. DOI: https://doi.org/10.2202/1544-6115.1128, PMID: 16646834

[69] Zhao W, Langfelder P, Fuller T, Dong J, Li A, Hovarth S. 2010. Weighted gene coexpression network analysis: state of the art. Journal of Biopharmaceutical Statistics 20:281–300. DOI: https://doi.org/10.1080/10543400903572753, PMID: 20309759

References

[1] Wilbrecht L, Nottebohm F. Vocal learning in birds and humans. Ment Retard Dev Disabil Res Rev. 2003;9(3):135-48. doi:10.100/mrdd.10073.

[2] Hauser MD, Chomsky N, Fitch WT. The faculty of language: what is it, who has it, and how did it evolve? Science. 2002; Nov 22;298(5598):1569-79. doi: 10.1126/science.298.5598.1569.

[3] Hurst JA, Baraitser M, Auger E, Graham F, Norell S. An extended family with a dominantly inherited speech disorder. Dev Med Child Neurol. 1990 Apr;32(4):352-5. PMID: 2332125.

[4] Gopnik M, Crago M. Familial aggregation of a developmental language disorder. Cognition. 1991 Apr;39(1):1-50. PMID: 1934976.

[5] Vargha-Khadem F, Watkins K, Alcock K, Fletcher P, Passingham R. Praxic and nonverbal cognitive deficits in a large family with a genetically transmitted speech and language disorder. Proc Natl Acad Sci U S A. 1995 Jan 31;92(3):930-3. PMID: 7846081.

[6] Fee EJ. The phonological system of a specifically language-impaired population. Clin Linguist Phon. 1995;9(3):189-209. doi: 10.3109/02699209508985332.

[7] Vargha-Khadem F, Gadian DG, Coop A, Mishkin M. FOXP2 and the neuroanatomy of speech and language. Nat Rev Neurosci. 2005 Feb;6(2):131-8. doi: 10.1038/nrn1605.

[8] Vargha-Khadem F, Watkins KE, Price CJ, Ashburner J, Alcock KJ, Connelly A, Frackowiak RS, Friston KJ, Pembrey ME, Mishkin M, Gadian DG, Passingham RE. Neural basis of an inherited speech and language disorder. Proc Natl Acad Sci U S A. 1998 Oct 13;95(21):12695-700. PMID: 9770548.

[9] Watkins KE, Gadian DG, Vargha-Khadem F. Functional and structural brain abnormalities associated with a genetic disorder of speech and language. Am J Hum Genet. 1999 Nov;65(5):1215-21. doi: 10.1086/302631.

[10] Belton E, Salmond CH, Watkins KE, Vargha-Khadem F, Gadian DG. Bilateral brain abnormalities associated with dominantly inherited verbal and orofacial dyspraxia. Hum Brain Mapp. 2003 Mar;18(3):194-200. doi: 10.1002/hbm.10093.

[11] Fisher S, Vargha-Khadem F, Watkins KE, Monaco AP, Pembrey ME. Localisation of a gene implicated in a severe speech and language disorder. Nat Genet. 1998 Feb;18(2):168-70. doi: 10.10338/ng0298-168.

[12] Bouffard GG, Idol JR, Braden VV, Iyer LM, Cunningham AF, Weintraub LA, Touchman JW, Mohr-Tidwell RM, Peluso DC, Fulton RS, Ueltzen MS, Weissenbach J, Magness

CL, Green ED. A physical map of human chromosome 7: an integrated YAC contig map with average STS spacing of 79kb. Genome Res. 1997 Jul;7(7):673-92. PMID: 9253597.

[13] Lai CS, Fisher SE, Hurst JA, Levy ER, Hodgson S, Fox M, Jeremiah S, Povey S, Jamison DC, Green ED, Vargha-Khadem F, Monaco AP. The SPCH1 region on human 7q31: genomic characterization of the critical interval and localization of translocations associated with speech and language disorder. Am J Hum Genet. 2000 Aug;67(2):357-68. doi: 10.1086/303011.

[14] Lai CS, Fisher SE, Hurst JA, Vargha-Khadem F, Monaco AP. A forkhead-domain gene is mutated in a severe speech and language disorder. Nature. 2001 Oct 4;413(6855):519-23. doi: 10.1038/35097076.

[15] Clark KL, Halay ED, Lai E, Burley SK. Co-crystal structure of the HNF-3/fork head DNA-recognition motif resembles histone H5. Nature. 1993 Jul 29;364(6436):412-20. doi: 10.1038/364412a0.

[16] Estruch SB, Graham SA, Quevedo M, Vino A, Dekkers DHW, Deriziotis P, Sollis E, Demmers J, Poot RA, Fisher SE. Proteomic analysis of FOXP proteins reveals interactions between cortical transcription factors associated with neurodevelopmental disorders. Hum Mol Genet. 2018 Jun 26. doi: 10.1093/hmg/ddy230.

[17] Li S, Weidenfeld J, Morrisey EE. Transcriptional and DNA binding activity of the Foxp1/2/4 family is modulated by heterotypic and homotypic protein interactions. Mol Cell Biol. 2004 Jan;24(2):809-22. PMID: 14701752.

[18] Shu W, Yang H, Zhang L, Lu MM, Morrisey EE. Characterization of a new subfamily of winged-helix/forkhead (Fox) genes that are expressed in the lung and act as transcriptional repressors. J Biol Chem. 2001 Jul 20;276(29):27488-97. doi: 10.1074/jbc.M100636200.

[19] Stroud JC, Wu Y, Bates DL, Han A, Nowick K, Paabo S, Tong H, Chen L. Structure of the forkhead domain of FOXP2 bound to DNA. Structure. 2006 Jan;14(1):159-66. doi: 10.1016/j.str.2005.10.005.

[20] Webb H, Steeb O, Blane A, Rotherham L, Aron S, Machanick P, Dirr H, Fanucchi S. The FOXP2 forkhead domain binds to a variety of DNA sequences with different rates and affinities. J Biochem. 2017 Jul 1;162(1):45-54. doi: 10.1093/jb/mvx003.

[21] Lai CS, Gerrelli D, Monaco AP, Fisher SE, Copp AJ. FOXP2 expression during brain development coincides with adult sites of pathology in a severe speech and language disorder. Brain. 2003 Nov;126(Pt 11):2455-62. doi: 10.1093/brain/awg247.

[22] Brainard MS, Doupe AJ. Translating birdsong: songbirds as a model for basic and applied medical research. Annu Rev Neurosci. 2013 Jul 8;36:489-517. doi: 10.1146/annurev-neuro-060909-152826.

[23] Doupe AJ, Kuhl PK. Birdsong and human speech: common themes and mechanisms. Annu Rev Neurosci. 1999;22:567-631. doi: 10.1146/annurev.neuro.22.1.567.

[24] Mooney R. Neurobiology of song learning. Curr Opin Neurobiol. 2009 Dec;19(6):654-60. doi: 10.1016/j.conb.2009.10.004.

[25] Pfenning AR, Hara E, Whitney O, Rivas MV, Wang R, Roulhac PL, Howard JT, Wirthlin M, Lovell PV, Ganapathy G, Mouncastle J, Moseley MA, Thompson JW, Soderblom EJ, Iriki A, Kato M, Gilbert MT, Zhang G, Bakken T, Bongaarts A, Bernard A, Lein E, Mello CV, Hartemink AJ, Jarvis ED. Convergent transcriptional specializations in the brains of humans and song-learning birds. Science. 2014 Dec 12;346(6215):1256846. doi: 10.1126/science.1256846.

[26] Teramitsu I, Kudo LC, London SE, Geschwind DH, White SA. Parallel FoxP1 and FoxP2 expression in songbird and human brain predicts functional interaction. J Neurosci. 2004 Mar 31;24(13):3152-63. doi: 10.1523/JNEUROSCI.5589-03.2004.

[27] Haesler S, Rochefort C, Georgi B, Licznerski P, Osten P, Scharff C. Incomplete and inaccurate vocal imitation after knockdown of FoxP2 in songbird basal ganglia nucleus Area X. PLoS Biol. 2007 Dec;5(12):e321. doi: 10.1371/journal.pbio.0050321.

[28] Heston JB, White SA. Behavior-linked FoxP2 regulation enables zebra finch vocal learning. J Neurosci. 2015 Feb 18;35(7):2885-94. doi: 10.1523/JNEUROSCI.3715-14.2015.

[29] Day N et al. In prep.

[30] Miller JE, Spiteri E, Condro MC, Dosumu-Johnson RT, Geschwind DH, White SA. Birdsong decreases protein levels of FoxP2, a molecule required for human speech. J Neurophysiol. 2008 Oct;100(4):2015-25. doi: 10.1152/jn.90415.2008.

[31] Miller JE, Hilliard AT, White SA. Song practice promotes acute vocal variability at a key stage of sensorimotor learning. PLoS One. 2010 Jan 6;5(1):e8592. doi: 10.1371/journal.pone.0008592.

[32] Zhang B, Horvath S. A general framework for weighted gene co-expression network analysis. Stat Appl Genet Mol Biol 2005; 4:Article17. doi:10.2202/1544-6115.1128.

[33] Hilliard AT, Miller JE, Horvath S, White SA. Distinct neurogenomic states in basal ganglia subregions relate differently to singing behavior in songbirds. PLoS Comput Biol. 2012;8(11):e1002773. doi: 10.1371/journal.pcbi.1002773.

[34] Hilliard AT, Miller JE, Fraley ER, Horvath S, White SA. Molecular microcircuitry underlies functional specification in a basal ganglia circuit dedicated to vocal learning. Neuron. 2012 Feb 9;73(3):537-52. doi: 10.1016/j.neuron.2012.01.005.

[35] Burkett ZD, Day NF, Kimball TH, Aamodt CM, Heston JB, Hilliard AT, Xiao X, White SA. FoxP2 isoforms delineate spatiotemporal transcriptional networks for vocal learning in the zebra finch. Elife. 2018 Jan 23;7. pii: e30649. doi: 10.7554/eLife.30649.

[36] Spiteri E, Konopka G, Coppola G, Bomar J, Oldham M, Ou J, Vernes SC, Fisher SE, Ren B, Geschwind DH. Identification of the transcriptional targets of FOXP2, a gene linked to speech and language, in developing human brain. Am J Hum Genet. 2007 Dec;81(6):1144-57. doi: 10.1086/522237.

[37] Vernes SC, Spiteri E, Nicod J, Groszer M, Taylor JM, Davies KE, Geschwind DH, Fisher SE. High-throughput analysis of promoter occupancy reveals direct neural targets of FOXP2, a gene mutated in speech and language disorders. Am J Hum Genet. 2007 Dec;81(6):1232-50. doi: 10.1086/522238.

[38] Vernes SC, Oliver PL, Spiteri E, Lockstone HE, Puliyadi R, Taylor JM, Ho J, Mombereau C, Brewer A, Lowy E, Nicod J, Groszer M, Baban D, Sahgal N, Cazier JB, Ragoussis J, Davies KE, Geschwind DH, Fisher SE. Foxp2 regulates gene networks implicated in neurite outgrowth in the developing brain. PLoS Genet. 2011 Jul;7(7):e1002145. doi: 10.1371/journal.pgen.1002145.

[39] Schmittgen TD, Livak KJ. Analyzing real-time PCR data by the comparative C(T) method. Nat Protoc. 2008;3(6):1101-8. PMID: 18546601

[40] Langmead B, Salzberg SL. Fast gapped-read alignment with Bowtie 2. Nat Methods. 2012 Mar 4;9(4):357-9. doi: 10.1038/nmeth.1923.

[41] Li H, Handsaker B, Wysoker A, Fennell T, Ruan J, Homer N, Marth G, Abecasis G, Durbin R; 1000 Genome Project Data Processing Subgroup. The Sequence Alignment/Map format and SAMtools. Bioinformatics. 2009 Aug 15;25(16):2078-9. doi: 10.1093/bioinformatics/btp352.

[42] Zhang Y, Liu T, Meyer CA, Eeckhoute J, Johnson DS, Bernstein BE, Nusbaum C, Myers RM, Brown M, Li W, Liu XS. Model-based analysis of ChIP-Seq (MACS). Genome Biol. 2008;9(9):R137. doi: 10.1186/gb-2008-9-9-r137.

[43] Lawrence M, Huber W, Pagès H, Aboyoun P, Carlson M, Gentleman R, Morgan MT, Carey VJ. Software for computing and annotating genomic ranges. PLoS Comput Biol. 2013;9(8):e1003118. doi: 10.1371/journal.pcbi.1003118.

[44] Bates D, Carey V, Dettling M, Dudoit S, Ellis B, Gautier L, Gentleman R, Gentry J, Hornik K, Hothorn T, Huber W, Iacus S, Irizarry R, Leisch F, Maechler M, Rossini A, Sawitzki G, Tierney L, Yang JYH, Zhang J. Bioconductor (Web Site), http://www.bioconductor.org/, 2002.

[45] Yates B, Braschi B, Gray KA, Seal RL, Tweedie S, Bruford EA. Genenames.org: the HGNC and VGNC resources in 2017. Nucleic Acids Res. 2017 Jan 4;45(D1):D619-D625. doi: 10.1093/nar/gkw1033.

[46] O'Leary NA, Wright MW, Brister JR, Ciufo S, Haddad D, McVeigh R, Rajput B, Robbertse B, Smith-White B, Ako-Adjei D, Astashyn A, Badretdin A, Bao Y, Blinkova O, Brover V, Chetvernin V, Choi J, Cox E, Ermolaeva O, Farrell CM, Goldfarb T, Gupta T, Haft D, Hatcher E, Hlavina W, Joardar VS, Kodali VK, Li W, Maglott D, Masterson P, McGarvey KM, Murphy MR, O'Neill K, Pujar S, Rangwala SH, Rausch D, Riddick LD, Schoch C, Shkeda A, Storz SS, Sun H, Thibaud-Nissen F, Tolstoy I, Tully RE, Vatsan AR, Wallin C, Webb D, Wu W, Landrum MJ, Kimchi A, Tatusova T, DiCuccio M, Kitts P, Murphy TD, Pruitt KD. Reference sequence (RefSeq) database at NCBI: current status, taxonomic expansion, and functional annotation. Nucleic Acids Res. 2016 Jan 4;44(D1):D733-45. doi: 10.1093/nar/gkv1189.

[47] Durinck S, Spellman PT, Birney E, Huber W. Mapping identifiers for the integration of genomic datasets with the R/Bioconductor package biomaRt. Nat Protoc. 2009;4(8):1184-91. doi: 10.1038/nprot.2009.97.

[48] Carlson M (2016). KEGG.db: A set of annotation maps for KEGG. R package version 3.2.3.

[49] Yu G, Wang LG, He QY. ChIPseeker: an R/Bioconductor package for ChIP peak annotation, comparison and visualization. Bioinformatics. 2015 Jul 15;31(14):2382-3. doi: 10.1093/bioinformatics/btv145.

[50] Khan A, Fornes O, Stigliani A, Gheorghe M, Castro-Mondragon JA, van der Lee R, Bessy A, Chèneby J, Kulkarni SR, Tan G, Baranasic D, Arenillas DJ, Sandelin A, Vandepoele K, Lenhard B, Ballester B, Wasserman WW, Parcy F, Mathelier A. JASPAR 2018: update of the open-access database of transcription factor binding profiles and its web framework. Nucleic Acids Res. 2018 Jan 4;46(D1):D1284. doi: 10.1093/nar/gkx1188.

[51] Pagès H, Aboyoun P, Gentleman R, DebRoy S (2018). Biostrings: Efficient manipulation of biological strings. R package version 2.48.0.

[52] Ramírez F, Dündar F, Diehl S, Grüning BA, Manke T. deepTools: a flexible platform for exploring deep-sequencing data. Nucleic Acids Res. 2014 Jul;42(Web Server issue):W187-91. doi: 10.1093/nar/gku365.

[53] Freese NH, Norris DC, Loraine AE. Integrated genome browser: visual analytics platform for genomics. Bioinformatics. 2016 Jul 15;32(14):2089-95. doi: 10.1093/bioinformatics/btw069.

[54] Adam I, Mendoza E, Kobalz U, Wohlgemuth S, Scharff C. CNTNAP2 is a direct FoxP2 target in vitro and in vivo in zebra finches: complex regulation by age and activity. Genes Brain Behav. 2017 Jul;16(6):635-642. doi: 10.1111/gbb.12390.

[55] Corona C, Pasini S, Liu J, Amar F, Greene LA, Shelanski ML. Activating Transcription Factor 4 (ATF4) Regulates Neuronal Activity by Controlling $GABA_BR$ Trafficking. J Neurosci. 2018 Jul 4;38(27):6102-6113. doi: 10.1523/JNEUROSCI.3350-17.2018.

[56] Sanz E, Yang L, Su T, Morris DR, McKnight GS, Amieux PS. Cell-type-specific isolation of ribosome-associated mRNA from complex tissues. Proc Natl Acad Sci U S A. 2009 Aug 18;106(33):13939-44. doi: 10.1073/pnas.0907143106.

[57] Adam I, Mendoza E, Kobalz U, Wohlgemuth S, Scharff C. FoxP2 directly regulates the reelin receptor VLDLR developmentally and by singing. Mol Cell Neurosci. 2016 Jul;74:96-105. doi: 10.1016/j.mcn.2016.04.002.